



THE UNIVERSITY *of* EDINBURGH

Edinburgh Research Explorer

Estimating Selection Intensity on Synonymous Codon Usage in a Nonequilibrium Population

Citation for published version:

Zeng, K & Charlesworth, B 2009, 'Estimating Selection Intensity on Synonymous Codon Usage in a Nonequilibrium Population', *Genetics*, vol. 183, no. 2, pp. 651-662.
<https://doi.org/10.1534/genetics.109.101782>

Digital Object Identifier (DOI):

[10.1534/genetics.109.101782](https://doi.org/10.1534/genetics.109.101782)

Link:

[Link to publication record in Edinburgh Research Explorer](#)

Document Version:

Publisher's PDF, also known as Version of record

Published In:

Genetics

Publisher Rights Statement:

Freely available via Pub Med.

General rights

Copyright for the publications made accessible via the Edinburgh Research Explorer is retained by the author(s) and / or other copyright owners and it is a condition of accessing these publications that users recognise and abide by the legal requirements associated with these rights.

Take down policy

The University of Edinburgh has made every reasonable effort to ensure that Edinburgh Research Explorer content complies with UK legislation. If you believe that the public display of this file breaches copyright please contact openaccess@ed.ac.uk providing details, and we will remove access to the work immediately and investigate your claim.



Estimating Selection Intensity on Synonymous Codon Usage in a Nonequilibrium Population

Kai Zeng^{*,†,1} and Brian Charlesworth^{*}

^{*}*Institute of Evolutionary Biology, School of Biological Sciences, University of Edinburgh, Edinburgh EH9 3JT, United Kingdom*
and [†]*State Key Laboratory of Biocontrol and Key Laboratory of Gene Engineering of the Ministry of Education, Sun Yat-Sen University, Guangzhou 510275, China*

Manuscript received February 13, 2009

Accepted for publication July 15, 2009

ABSTRACT

Codon usage bias is the nonrandom use of synonymous codons for the same amino acid. Most population genetic models of codon usage evolution assume that the population is at mutation–selection–drift equilibrium. Natural populations, however, frequently deviate from equilibrium, often because of recent demographic changes. Here, we construct a matrix model that includes the effects of a recent change in population size on estimates of selection on preferred *vs.* unpreferred codons. Our results suggest that patterns of synonymous polymorphisms affecting codon usage can be quite erratic after such a change; statistical methods that fail to take demographic effects into account can then give incorrect estimates of important parameters. We propose a new method that can accurately estimate both demographic and codon usage parameters. The method also provides a simple way of testing for the effects of covariates such as gene length and level of gene expression on the intensity of selection, which we apply to a large *Drosophila melanogaster* polymorphism data set. Our analyses of twofold degenerate codons reveal that (i) selection acts in favor of preferred codons, (ii) there is mutational bias in favor of unpreferred codons, (iii) shorter genes and genes with higher expression levels are under stronger selection, and (iv) there is little evidence for a recent change in population size in the Zimbabwe population of *D. melanogaster*.

CODONS specifying the same amino acid are called synonymous codons. These are often used nonrandomly, with some codons appearing more frequently than others. This biased usage of synonymous codons has been found in many organisms such as *Drosophila*, yeast, and bacteria (IKEMURA 1985; DURET and MOUCHIROUD 1999; HERSHBERG and PETROV 2008). Conventionally, synonymous codons for a given amino acid are divided into two classes: preferred and unpreferred codons (IKEMURA 1985; AKASHI 1994; DURET and MOUCHIROUD 1999). Several observations indicate that codon usage is affected by natural selection. First, in species with codon usage bias, preferred codons generally correspond to the most abundant tRNA species (IKEMURA 1981). Second, highly expressed genes usually have higher codon usage bias than genes with low expression (SHARP and LI 1986; DURET and MOUCHIROUD 1999; HEY and KLIMAN 2002). Third, the synonymous substitution rate of a gene has been shown to be negatively correlated with its degree of codon usage bias (SHARP and LI 1986; BIERNE and EYRE-WALKER 2006). The most commonly cited explanations

of the apparent fitness differences between preferred and unpreferred codons are selection for translation efficiency, translational accuracy, and mRNA stability (IKEMURA 1985; EYRE-WALKER and BULMER 1993; AKASHI 1994; DRUMMOND *et al.* 2005). Recently, it has been proposed that exon splicing also affects codon usage bias (WARNECKE and HURST 2007).

From a population genetics perspective, the extent of codon usage bias is ultimately a product of the joint effects of mutation, selection, genetic drift, recombination, and demographic history. The Li–Bulmer model of drift, selection, and reversible mutation between preferred and unpreferred codons at a site is the most widely used model (LI 1987; BULMER 1991; McVEAN and CHARLESWORTH 1999). Applications of this model generally assume that the population is at mutation–selection–drift equilibrium. However, empirical studies have suggested that changes in the strengths of various driving forces may not be unusual. For example, in *Drosophila melanogaster*, there is evidence that the population size (LI and STEPHAN 2006; THORNTON and ANDOLFATTO 2006; KEIGHTLEY and EYRE-WALKER 2007; STEPHAN and LI 2007), recombinational landscape (TAKANO-SHIMIZU 1999), and mutational process (TAKANO-SHIMIZU 2001; KERN and BEGUN 2005) may have changed significantly over the species' evolutionary history.

Supporting information is available online at <http://www.genetics.org/cgi/content/full/genetics.109.101782/DC1>.

¹*Corresponding author:* Institute of Evolutionary Biology, School of Biological Sciences, University of Edinburgh, Ashworth Laboratories, King's Bldgs., W. Mains Rd., Edinburgh EH9 3JT, United Kingdom.
E-mail: kai.zeng.cn@gmail.com

Such changes cause departures from equilibrium. Theoretical models show that it takes a very long time, proportional to the reciprocal of the mutation rate, for the population to approach a new equilibrium state (TACHIDA 2000; COMERON and KREITMAN 2002). Before reaching equilibrium, the population often shows counterintuitive patterns of evolution (EYRE-WALKER 1997; TAKANO-SHIMIZU 1999, 2001; COMERON and KREITMAN 2002; COMERON and GUTHRIE 2005; CHARLESWORTH and EYRE-WALKER 2007). Despite these theoretical results, details of the patterns of polymorphism and substitution rates following a recent change in population size, and their effects on estimates of strength of selection, have not been determined.

The above findings point to the importance of incorporating nonequilibrium factors into the study of codon usage bias. To this end, we extend the Li-Bulmer model to allow population size to vary over time, by representing the evolutionary process by a transition matrix. By analyzing this matrix model, we show that a recent change in population size can result in erratic patterns of codon usage and that methods failing to take into account these demographic effects can give false estimates of the intensity of selection.

To solve these problems, we propose a new method, which does not require polarizing ancestral *vs.* derived states using outgroup data (*cf.* CUTTER and CHARLESWORTH 2006), but requires only knowledge of preferred *vs.* unpreferred states defined by patterns of codon usage. We use information on both polymorphic and fixed sites, which enables both mutational bias and the strength of selection to be estimated, in contrast to previous methods that use information on polymorphisms alone. Simulations indicate that this method can accurately estimate both demographic and codon usage parameters and can distinguish between selection and demography. We use the new method to analyze a large *D. melanogaster* polymorphism data set (SHAPIRO *et al.* 2007) and find evidence for natural selection on synonymous codons. We use our approach to show that genes with shorter coding sequences and higher levels of expression are under significantly stronger selection than longer genes with lower expression.

MATERIALS AND METHODS

Description of the model: We consider a diploid Wright-Fisher population (EWENS 2004, p. 21), whose size in generation t is N_t . At an autosomal nucleotide site, two variants, A and a , can occur. Mutation is reversible: the per generation mutation rate from a to A is u , and the rate in the opposite direction is κu . The fitnesses of the three possible genotypes, AA , Aa , and aa are 1, $1 - \frac{1}{2}s$, and $1 - s$, respectively (the genic selection model). Denote the number of occurrences of allele A in generation t by $X(t)$. If $X(t) = i$, and assuming that mutation precedes selection, the frequency of A after mutation is

$$x^*(t) = \frac{i}{2N_t}(1 - \kappa u) + \left(1 - \frac{i}{2N_t}\right)u. \quad (1)$$

After selection, this becomes

$$x(t) = \frac{x^*(t)[1 - (1/2)s(1 - x^*(t))]}{1 - s(1 - x^*(t))}. \quad (2)$$

The transition probability for $X(t)$ is thus

$$\begin{aligned} p_{ij}(t) &= \Pr\{X(t+1) = j | X(t) = i\} \\ &= \binom{2N_{t+1}}{j} (x(t))^j (1 - x(t))^{2N_{t+1}-j}. \end{aligned} \quad (3)$$

In Equations 1–3, we have $0 \leq i \leq 2N_t$ and $0 \leq j \leq 2N_{t+1}$.

Let $f_j(t) = \Pr(X(t) = j)$ be the probability that A is represented j times in the population at time t . This satisfies the relation

$$\sum_{j=0}^{2N_t} f_j(t) = 1. \quad (4)$$

Standard Markov chain theory (KARLIN and TAYLOR 1975) implies the recursion relationship

$$f_j(t+1) = \sum_{i=0}^{2N_t} f_i(t)p_{ij}(t), \quad 0 \leq j \leq 2N_{t+1}. \quad (5)$$

In an equilibrium population with constant size N , Equation 5 can be written as

$$f_j = \sum_{i=0}^{2N} f_i p_{ij}, \quad 0 \leq j \leq 2N. \quad (6)$$

Equation 6 is a system of linear equations subject to the requirement given in Equation 4.

Following the method used to calculate the frequency spectrum of polymorphic sites under the infinite-sites model (*e.g.*, Equation 16 in McVEAN and CHARLESWORTH 1999), we can decompose $f_j(t)$ into two subprocesses:

$$f_j(t) = f_{A,j}(t) + f_{a,2N_t-j}(t), \quad 1 \leq j \leq 2N_t - 1. \quad (7)$$

Here, $f_{A,j}(t)$ is the probability that the mutant allele A is currently represented j times in the population, having originated at a site fixed for a . We call these mutations “ $a \rightarrow A$ polymorphic mutations.” The second subprocess involves mutations originating at sites fixed for A , such that the mutant allele a is currently represented $2N_t - j$ times in the population (*i.e.*, A is represented j times); these are $A \rightarrow a$ polymorphic mutations. For the first subprocess, we have the following recursion formula

$$\begin{aligned} f_{A,j}(t+1) &= \sum_{i=1}^{2N_t-1} f_{A,i}(t)p_{ij}(t) + f_0(t)p_{0j}(t), \quad 1 \leq j \leq 2N_{t+1} - 1. \end{aligned} \quad (8)$$

The first term on the right describes the dynamics of sites that are polymorphic in the t th generation, and the second term describes new $a \rightarrow A$ polymorphic mutations. This formula is analogous to Equation 3 of EVANS *et al.* (2007), which was derived under the infinite-sites model. A similar formula holds for the second subprocess. Equations 7 and 8 provide an alternative way of calculating the frequency spectrum of polymorphic sites, on the infinite-sites assumption that all new mutations arise at sites that are fixed for either A or a ; but in fact they apply more generally. Some examples are given in

supporting information, Figure S1. While the application of our model to data analysis does not depend critically on the infinite-sites assumption, this is likely to be a good approximation in practice and is valid for the simulations described in the first part of the RESULTS section.

From the two subprocesses, the proportion of polymorphic sites originating from sites previously fixed for a , P_a , is given by

$$P_a(t) = \frac{\sum_{j=1}^{2N_t-1} f_{A,j}(t)}{\sum_{j=1}^{2N_t-1} (f_{A,j}(t) + f_{a,j}(t))}. \quad (9)$$

The proportion of polymorphic sites that originated from sites previously fixed for A , P_A , can be calculated similarly. Furthermore, we can calculate the rate at which a site currently fixed for a is replaced by a site fixed for A , denoted by $r_{aA}(t)$:

$$r_{aA}(t) = \sum_{j=1}^{2N_{t-1}-1} f_{A,j}(t-1) p_{j,2N_t}(t-1) + f_0(t-1) p_{0,2N_t}(t-1). \quad (10)$$

Similarly, we can calculate the rate, $r_{AA}(t)$, at which a site currently fixed for A is replaced by a site fixed for a . Thus, the total substitution rate is

$$r(t) = r_{aA}(t) + r_{AA}(t). \quad (11)$$

In an equilibrium population, Equations 7–11 are independent of t .

Statistical methods: In this section, we use the theory developed above to construct two new methods that are based on the frequencies of preferred *vs.* unpreferred variants at nucleotide sites and do not require the use of an outgroup to infer ancestral *vs.* derived states, extending the similar approach of CUTTER and CHARLESWORTH (2006). Let d_i be the number of sites at which allele A is represented i times in a sample of n alleles from a population. The frequency distribution for the sample, \mathbf{d} , is a vector of all the d_i 's ($0 \leq i \leq n$); this includes cases where the sample is fixed for either A or a .

We start with the simple case where the population is at equilibrium, denoted as L_0 . The population dynamics are determined by the parameters N , u , κ , and s . However, if all evolutionary forces are weak so that the diffusion approximation holds, the state of a sample from the population is described by the compound parameters $\theta = 4Nu$ and $\gamma = 2Ns$ (EWENS 2004, Chap. 5). The distribution of the numbers of copies of A per site in the population can be calculated by solving Equation 6 numerically (see below). We write this distribution as \mathbf{f} , which is a vector with $2N + 1$ elements. The log-likelihood for the sample, \mathbf{d} , is the

$$L_0(\mathbf{d} | \gamma, \theta, \kappa) = \sum_{i=0}^n d_i \times \log \left[\sum_{j=0}^{2N} f_j \binom{n}{i} \left(\frac{j}{2N} \right)^i \left(1 - \frac{j}{2N} \right)^{n-i} \right]. \quad (12)$$

In Equation 12, we have adopted the “conventional” assumption that sites behave independently of each other (AKASHI and SCHAEFFER 1997; EYRE-WALKER 1997; McVEAN and VIEIRA 1999; McVEAN and CHARLESWORTH 2000; MASIDE *et al.* 2004; CUTTER and CHARLESWORTH 2006; GALTIER *et al.* 2006). Although this assumption is unrealistic, it is mathematically tractable and seems to work fairly well in practice with relatively free recombination (*e.g.*, with a local recombination rate >2 cM/Mb, K. ZENG, unpublished results; see also WILLIAMSON *et al.* 2005 and BOYKO *et al.* 2008).

To model the effects of a change in population size, we assume that the population is originally at equilibrium with population size N_b . Its population size then changes instantly

to N_a and stays constant for t generations, at which point a sample is taken from the population. Hence, the model, denoted as L_1 , has five parameters: $\gamma_b (= 2N_b s)$, $\theta_b (= 4N_b u)$, κ , $g (= N_a/N_b)$, and $\tau (= t/N_a)$. The demographic model underlying L_1 , although somewhat unrealistic, is mathematically tractable and has been widely used (WILLIAMSON *et al.* 2005; LI and STEPHAN 2006; KEIGHTLEY and EYRE-WALKER 2007; BOYKO *et al.* 2008).

Let the distribution of the numbers of A per site in the generation just before the change in population size be \mathbf{f}^b . Then the distribution in the t th generation after the change, $\mathbf{f}^a(t)$ (a vector with $2N_a + 1$ elements), can be obtained by iterating Equation 5 with \mathbf{f}^b as the initial condition. The log-likelihood of the data is now

$$L_1(\mathbf{d} | \gamma_b, \theta_b, \kappa, g, t) = \sum_{i=0}^n d_i \times \log \left[\sum_{j=0}^{2N_a} f_j^a(t) \binom{n}{i} \left(\frac{j}{2N_a} \right)^i \left(1 - \frac{j}{2N_a} \right)^{n-i} \right]. \quad (13)$$

Note that, when $g = 1$ and/or $\tau = \infty$, the more complex model, $L_1(\mathbf{d} | \gamma_b, \theta_b, \kappa, g, t)$, reduces to the simpler model, $L_0(\mathbf{d} | \gamma, \theta, \kappa)$. Here, following WILLIAMSON *et al.* (2005), we use a chi-square test with 2 d.f. to distinguish these two models under the assumption that it will yield a conservative test.

Numerical computations: We used standard numerical methods to solve the linear system given in Equation 6: an LU-decomposition procedure followed by one round of numerical improvement (PRESS *et al.* 1992). The adequacy of this numerical method was checked by comparing the results with those obtained by iterating Equation 5 (results not shown). To find the maximum-likelihood estimates (MLEs) of the parameters, we used the simplex algorithm (PRESS *et al.* 1992). Multiple start points were used to make sure that the global maximum was found. To save computer time, we used a relatively loose search criterion in the simulations, with a sparse grid of values and a relaxed convergence criterion.

When implementing the model, the size of the transition matrix has to be specified. As mentioned above, population dynamics in the diffusion limit are determined by the compound parameters θ and γ . Hence it is legitimate to “scale down” the population size to give a tractable size of matrix, preserving the θ - and γ -values for the true population size. This rescaling has been widely used in population genetics (McVEAN and CHARLESWORTH 2000; TACHIDA 2000; COMERON and KREITMAN 2002; KEIGHTLEY and EYRE-WALKER 2007; KAISER and CHARLESWORTH 2009). In our own experience, rescaling produced reasonable results even when N was set to 10 (see Table S1).

When computing the more complex model given in Equation 13, it was not feasible to use the simplex algorithm to examine the full domain of g [*i.e.*, $g \in (0, \infty)$], so we restricted the search to $g \in (0.05, 20)$.

Simulation methods: To generate a random sample of size n under the constant population size model (L_0), we first solved Equation 6 numerically to obtain \mathbf{f} . We then determined the population frequency of A , denoted as x , by sampling from \mathbf{f} . Finally we obtained the number of copies of A in a sample of size n by drawing from a binomial distribution with parameters n and x . A similar procedure was used to generate random samples under the more complex model (L_1).

Source of data: We applied these methods to a large *D. melanogaster* polymorphism data set (SHAPIRO *et al.* 2007). The data, which were kindly provided by D. Turissini, contained alignments of 468 autosomal loci. A number of Zimbabwe and cosmopolitan lines were sampled. We used only the Zimbabwe

TABLE 1

Summary of the *D. melanogaster* polymorphism data

G^a	\bar{n}^b	L^c	S^d	θ_W^e	θ_π^f	Tajima's D^g
182	5.5	14,807	335	0.0107	0.0108	-0.0076

^aTotal number of loci.^bMean sample size.^cTotal number of twofold degenerate sites.^dTotal number of polymorphic twofold degenerate sites.^eMean value of Watterson's estimator of (per site) population mutation rate (WATTERSON 1975). In the calculation, only twofold degenerate sites were used.^fMean nucleotide diversity. In the calculation, only twofold degenerate sites were used.^gMean Tajima's D statistic (TAJIMA 1989). In the calculation, only twofold degenerate sites were used.

lines in our analysis because of severe bottleneck effects in the other population that was sampled (GLINKA *et al.* 2003; HADDRILL *et al.* 2005; LI and STEPHAN 2006; THORNTON and ANDOLFATTO 2006). Among the Zimbabwe lines, we used only those showing the strongest evidence for reproductive isolation, the "strong Z lines." This avoids the possibility that the Z lines with reduced reproductive isolation with the cosmopolitan lines might have been formed by secondary contact with the cosmopolitan lines; these gave an excess of intermediate-frequency variants in the frequency spectrum when these "weak" Z lines were included in the analysis (J. SHAPIRO and C.-I. WU, personal communication).

To annotate the data, we downloaded version 5.11 of the *D. melanogaster* genome data from FlyBase (<http://flybase.org/>). We then used BLAT (version 34, with default parameters; <http://genome-test.cse.ucsc.edu/~kent/exe/linux/>) to align the data to the reference genome. We excluded eight loci falling into putatively repetitive regions and one locus falling into a heterochromatic region. For the other loci, we used their genomic locations to obtain estimates of local recombination rate using a well-established method (SINGH *et al.* 2005) (the data were available online from the Petrov laboratory at http://petrov.stanford.edu/cgi-bin/recombination-rates_updateR5.pl). To reduce the effect of linkage, we analyzed only loci locating in highly recombining regions, defined as regions with a local recombination rate strictly >2.3 cM/Mb (SINGH *et al.* 2005). To avoid the complication of alternatively spliced genes (IDA and AKASHI 2000), we retained only loci overlapping one annotated well-defined coding region (*i.e.*, starting with a start codon, ending with a stop codon, and possessing no premature stop codon). We further excluded codons where mutations in the first position could change the status of the third codon position (*e.g.*, from fourfold degenerate to twofold degenerate). Insertions and deletions were also removed. For the genes passing all the above filters, we extracted twofold degenerate codons and defined preferred/unpreferred codons as in DURET and MOUCHIROUD (1999). A summary of the data is given in Table 1.

RESULTS

Effects of a change in population size on patterns of codon usage evolution: In this section, we assumed that the population size changed instantly from N_b to N_a at time zero and stayed constant thereafter. Allele A was

the preferred allele, but mutation was biased toward the unpreferred allele, a (*i.e.*, $\kappa > 1$). First, we explored the effects of population expansion by assuming that the population size instantly increased 10-fold at time zero (*i.e.*, $N_a = 10N_b$; Figure 1). As reported previously (TAKANO-SHIMIZU 1999; CHARLESWORTH and EYRE-WALKER 2007), for a long period after the expansion ($\sim 38N_a$ generations in Figure 1A), the total substitution rate is higher than that before the expansion. This is due to a sharp increase in r_{aA} (the top curve in Figure 1A). Patterns of polymorphism are also complex (Figure 1B). For example, the frequency of polymorphisms arising from sites fixed for a (P_a) first increases and then gradually decreases to its new equilibrium level. This behavior of P_a is caused by the following dynamics. Just after the expansion, there are many more sites fixed for a in the population than at equilibrium under the new, larger population size. With the parameter values used in Figure 1, 68% of the sites are expected to be fixed for a before the expansion, whereas this number decreases to 12% under the new population size. Thus, immediately after the expansion, the chance of occurrence of an $a \rightarrow A$ mutation is higher than at equilibrium with the new population size. On the other hand, the population expansion changes the scaled selection coefficient from $\gamma_b = 2N_b s = 0.3$, the value before the change, to $\gamma_a = 2N_a s = 3$, the value after the change. As a result, under the new population size, $A \rightarrow a$ polymorphic mutations become more deleterious and are more efficiently purged, whereas $a \rightarrow A$ polymorphic mutations become more advantageous and are more likely to escape stochastic loss and to segregate at an appreciable frequency. These nonequilibrium dynamics lead to the transient increase in P_a . However, as time elapses, the number of sites fixed for a gradually decreases, and P_a also slowly decreases to its new equilibrium value.

Another feature of Figure 1B is of interest: for $\sim 5N_a$ generations $P_a \geq P_A$. This observation is striking because (i) $P_A = P_a = 50\%$, which occurs twice in Figure 1B when the two curves intersect, is a pattern expected under an equilibrium population with neutrality (MCVEAN and CHARLESWORTH 1999) and (ii) $P_a > P_A$ is expected under an equilibrium model when a is preferred (MCVEAN and CHARLESWORTH 1999), but here a was unpreferred. These results strongly suggest that using predictions made by equilibrium models of codon usage to interpret patterns of polymorphism observed in a nonequilibrium population may lead to very misleading conclusions.

Next, we examined the effects of a reduction in population size. In Figure 2, a 10-fold decrease was assumed (*i.e.*, $10N_a = N_b$). Immediately after the reduction, the total substitution rate, r , is much higher than that before (Figure 2A), consistent with previous results (TAKANO-SHIMIZU 1999; CHARLESWORTH and EYRE-WALKER 2007). The increase in r is due to in-

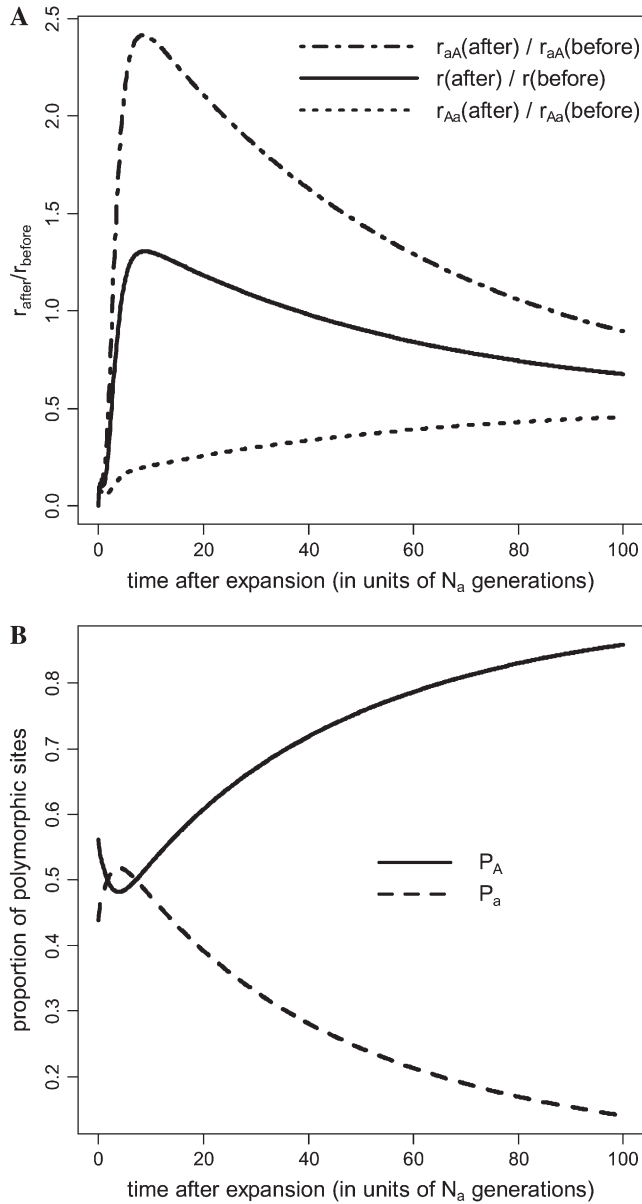


FIGURE 1.—Patterns of substitution and polymorphism after a recent population size expansion. We assumed that a diploid population of size N_b was originally at equilibrium. At time zero the population size increased instantly 10-fold to N_a and stayed constant thereafter. Allele A was assumed to be the preferred allele. The parameters used were $\gamma_b = 2N_b s = 0.3$, $\theta_b = 4N_b u = 0.002$, and $\kappa = 3$. Time was measured in units of N_a generations. (A) Patterns of substitution. We calculated three quantities: r_{aA} (the rate at which sites fixed for allele a were replaced by sites fixed for allele A ; see Equation 10), r_{Aa} (the rate at which sites fixed for A were replaced by sites fixed for a), and $r = r_{aA} + r_{Aa}$, the total substitution rate. Shown are the ratios of the values of these quantities after the change in population size to their equilibrium values before the change. (B) Patterns of polymorphism. P_A (or P_a) is the proportion of polymorphic sites originating from sites previously fixed for A (or a) (see Equation 9).

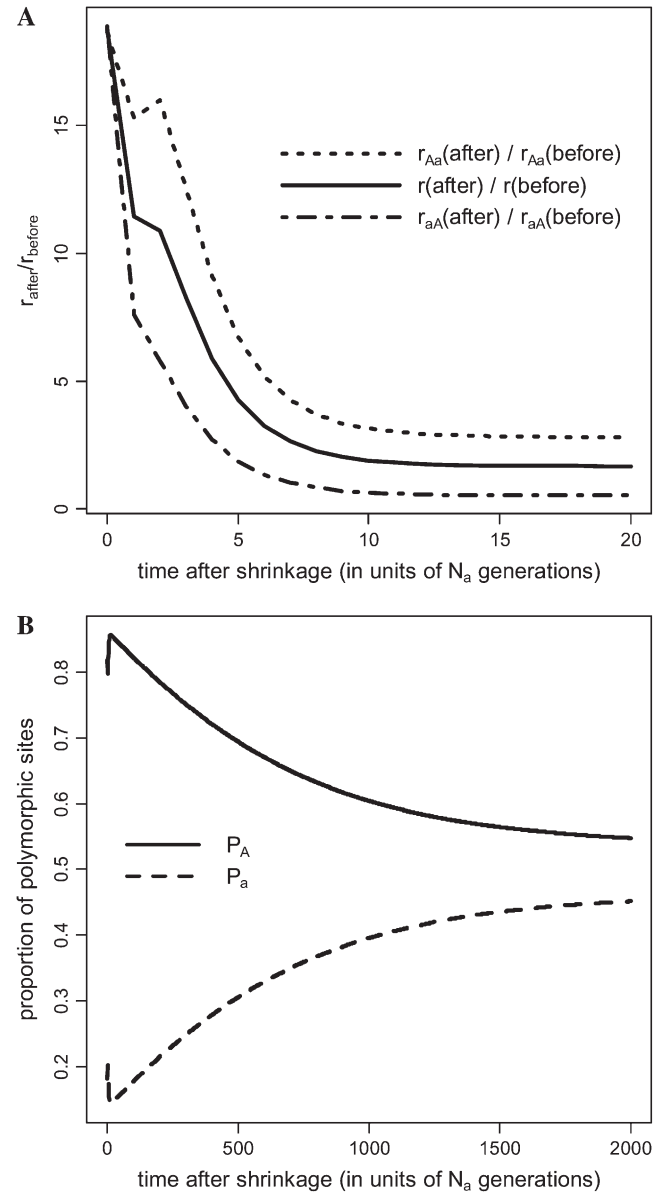


FIGURE 2.—Patterns of substitution and polymorphism after a recent population size shrinkage. We assumed that a diploid population of size N_b was originally at equilibrium. At time zero the population size decreased instantly 10-fold to N_a and stayed constant thereafter. Allele A was assumed to be the preferred allele. The parameters used were $\gamma_b = 2$, $\theta_b = 0.02$, and $\kappa = 3$. Time was measured in units of N_a generations. (A) Pattern of substitution. (B) Pattern of polymorphism. Definitions of the quantities r_{aA} , r_{Aa} , r , P_A , and P_a are the same as those given in Figure 1.

creases in both r_{Aa} and r_{aA} . Patterns of polymorphism also show interesting dynamics. Before reaching their new equilibrium values of 54 and 46%, respectively, the difference between P_A and P_a increases temporarily (Figure 2B), mimicking an increase in selection pressure on synonymous codons, despite the fact that the selection pressure is greatly reduced due to the sharp decrease in population size. This increased difference between P_A and P_a is caused by (i) a transient increase

in the number of sites fixed for A (see Figure S2), which allows more $A \rightarrow a$ polymorphic mutations to occur, and (ii) a decrease in the total number of $a \rightarrow A$ mutations arising each generation. Interestingly, the transient increase in the number of sites fixed for A also results in a brief increase in r_{Aa} at $\sim 2N_a$ generations after the contraction.

In brief, the dynamics of codon usage can be rather complex following a recent change in population size. Patterns of polymorphism may imitate those expected under a weaker (Figure 1B) or a stronger (Figure 2B) selection pressure on synonymous codons. Further, these misleading patterns can persist for long periods, as the time required for the population to reach the new equilibrium state is typically very long (*e.g.*, Figures 1 and 2).

The effects of a recent population size change on methods that assume equilibrium: A number of methods have been proposed to quantify the selection pressure on synonymous codons using within-species polymorphism data (AKASHI and SCHAEFFER 1997; MASIDE *et al.* 2004; COMERON and GUTHRIE 2005; CUTTER and CHARLESWORTH 2006). These methods assume that the population is at mutation–selection–drift equilibrium. However, given the results described above, knowing the performance of these methods in a nonequilibrium population is important. To this end, we used the method of MASIDE *et al.* (2004) as an example, due to its simplicity in calculation. This method relies on some well-established diffusion approximations (MCVEAN and CHARLESWORTH 1999). Our simulations suggest that when the population is at equilibrium and there is mutational bias, the method may give slightly biased estimates of γ , but this is apparent only when selection is very weak (see Figure S3).

In Figure 3, the same model and parameters used to obtain Figure 1 were used to generate random samples of size 15 with 10,000 codons at various time points after the population expansion. We used the MASIDE *et al.* (2004) method to analyze these samples. As shown by Figure 3A, the mean value of the maximum-likelihood estimate (mean MLE) of γ starts at a value ~ 0.3 , the true value before the expansion, and then goes down to a value of ~ -0.5 ; thereafter, the mean MLE increases monotonically toward the new equilibrium value of 3. Over this time period, the mean MLE of γ takes the value of zero twice, at $\sim N_a$ and $\sim 16N_a$ generations after the expansion, respectively. These two special time points correspond to the two occasions when $P_A = P_a = 50\%$ in Figure 1B. The power of the method to reject neutrality at a significance level of 5% is shown in Figure 3B. There are two dips in the power curve. Not surprisingly, these two significant reductions in power occur when the mean MLE of γ takes the value of zero. One feature of special note in Figure 3 is that, during the time between the two occasions when the mean MLE of γ is zero, the MASIDE *et al.* (2004) method has great power to reject neutral

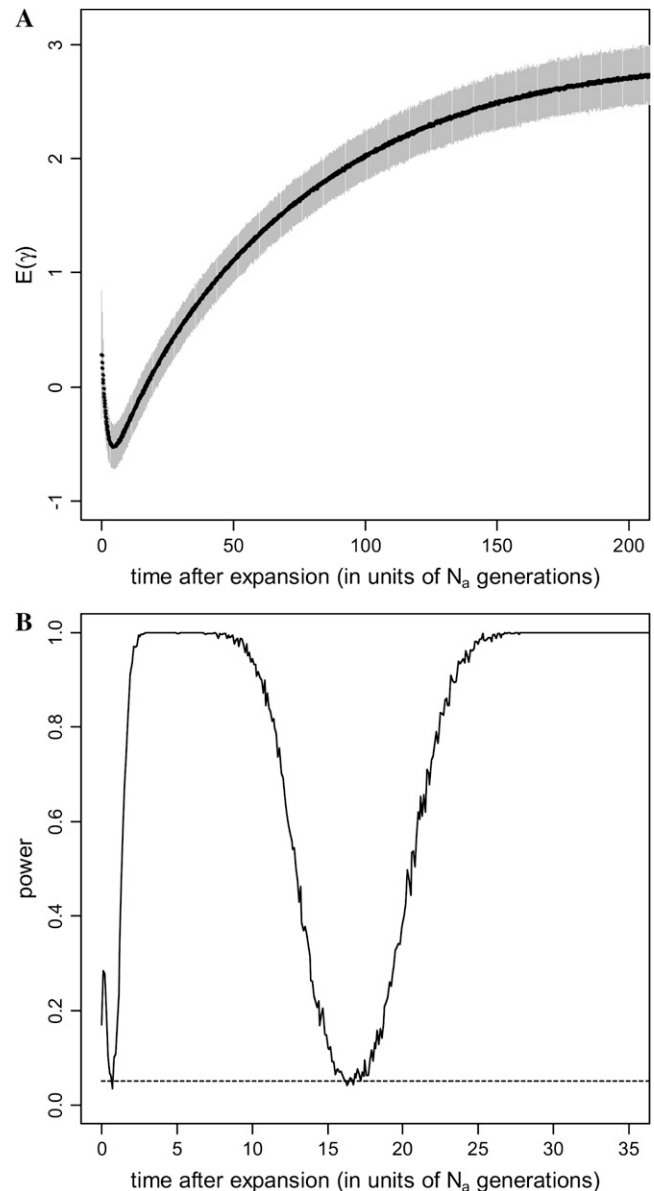


FIGURE 3.—Effects of a recent population size expansion on the MASIDE *et al.* (2004) method. The model and parameters used were the same as those used to generate Figure 1 (*i.e.*, a 10-fold increase in population size, $\gamma_b = 0.3$, $\theta_b = 0.002$, and $\kappa = 3$). At each time point after the expansion in population size, we randomly generated 500 samples. Each sample was composed of 15 sequences of 10,000 codons. We then used the MASIDE *et al.* (2004) method to analyze these samples and obtained a distribution of estimated γ . (A) The solid curve shows the mean value of the estimates of γ , and the shaded sleeve indicates where 95% of the probability mass of the distribution lies. (B) The power of the Maside *et al.* method to reject neutrality at a significance level of 5%. Note that the timescale is different in the two plots.

evolution for the data sets that we simulated. However, the γ -value that the method returns has, on average, a different sign from the true value. In other words, the preferred/unpreferred state estimated by the method is the reverse of the true situation. Further investigation

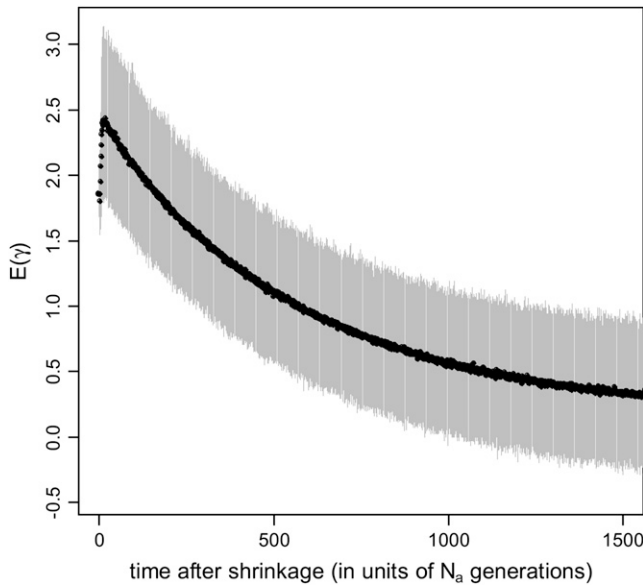


FIGURE 4.—Effects of a recent population size reduction on the MASIDE *et al.* (2004) method. The model and parameters used were the same as those used to generate Figure 2 (*i.e.*, a 10-fold decrease in population size, $\gamma_b = 2$, $\theta_b = 0.02$, and $\kappa = 3$). At each time point after the reduction in population size, we randomly generated 500 samples. Each sample was composed of 15 sequences of 10,000 codons. We then used the Maside *et al.* method to analyze these samples and obtained a distribution of estimated γ . The solid curve shows the mean of the estimates of γ , and the shaded sleeve indicates where 95% of the probability mass of the distribution lies.

suggests that the negative mean MLE was not caused by our incorporation of a strong mutational bias in the simulation ($\kappa = 3$), because the same pattern was observed when κ was set to one (results not shown).

In agreement with the results shown in Figure 2B, there is a brief increase in the mean MLE of γ immediately after a reduction in population size (Figure 4), and thereafter the mean MLE decreases steadily toward the new equilibrium value of 0.2. The power of the Maside *et al.* method to reject neutrality in this case is a monotonically decreasing function of time (see Figure S4).

We also carried out simulations to examine effects of nonequilibrium evolution on the Akashi–Schaeffer method (AKASHI and SCHAEFFER 1997; see Figure S8 and Figure S9) and the Cutter–Charlesworth method (CUTTER and CHARLESWORTH 2006; see Figure S10 and Figure S11). Both methods are affected. Interestingly, the Akashi–Schaeffer method overestimates the intensity of selection after a population size expansion and falsely infers the sign of γ after a population size reduction; these patterns are the reverse of those for the Maside *et al.* method. The Cutter–Charlesworth method has similar properties to the Maside *et al.* method.

Taken together, the results suggest that recent population size changes can cause methods that assume equilibrium to give misleading results. First, the esti-

mated selection pressure on synonymous codons may be very different from the true value (Figures 3A and 4); second, neutrality may be falsely accepted (Figure 3B).

The performance of the new estimation methods: To model the effects of a change in population size with the new methods described in MATERIALS AND METHODS, we constructed two statistical models: L_0 and L_1 . L_0 assumes that the population is at equilibrium and has three parameters: γ , θ , and κ . L_1 assumes that the population is originally at equilibrium with population size N_b . Then the population size changes instantly to N_a and stays constant thereafter for t generations, at which point a sample is taken from the population. Hence, L_1 has five parameters: $\gamma_b (= 2N_b s)$, $\theta_b (= 4N_b u)$, κ , $g (= N_a/N_b)$, and $\tau (= t/N_a)$.

In contrast to previous methods, which do not estimate mutational parameters (AKASHI and SCHAEFFER 1997; MASIDE *et al.* 2004; COMERON and GUTHRIE 2005; CUTTER and CHARLESWORTH 2006), L_0 simultaneously estimates mutational (θ and κ) and selection (γ) parameters. Simulation results show that L_0 has high accuracy in estimating all the parameters (Table 2). However, similarly to the Maside *et al.* method, L_0 is susceptible to violation of the equilibrium assumption (see Figure S5 and Figure S6). In this case, the behavior of L_0 is rather similar to that of the Maside *et al.* method: following a recent population expansion the mean MLE of γ first decreases and then slowly increases to the new equilibrium value. The difference is that the mean MLE of γ returned by L_0 takes a minimum value of ~ 0.1 and never becomes negative. Estimates of κ and θ produced by L_0 are also likely to be biased by recent demographic changes (see Figure S5 and Figure S6).

The L_1 method has two more parameters, τ and g , and requires the iteration of Equation 5. Hence, L_1 is the most computationally intense method considered here. Again we did simulations to examine the properties of L_1 (Table 3). The accuracy of L_1 in estimating the parameters is generally quite high. Importantly, the method seems to have good power to reject a model with constant population size and to detect selection (Table 3). However, when only a relatively small amount of data is available, the accuracy and power of the L_1 method are reduced (see the second set of results in Table 3). In this case, the model with a recent population size reduction seems to be particularly problematic: in the simulations, the simplex algorithm we used often failed to converge and returned unrealistic results. Interestingly, reducing the amount of data does not reduce the power of the method to detect selection if the population size is declining, whereas a limited amount of data does reduce the power to detect selection if the population size is increasing. This difference is probably caused by the fact that immediately after a reduction in population size, patterns of

TABLE 2
Performance of the L_0 method in an equilibrium population

	θ	κ	γ
Sample size = 15, no. of codons per sequence = 10,000			
Input ^a	0.01	1	0
Mean MLE ^b	0.01	1.02	-0.0009
Percentiles ^c	[0.008, 0.012]	[0.71, 1.45]	[-0.3772, 0.3488]
Input ^a	0.01	3	1
Mean MLE ^b	0.01	3.01	1.02
Percentiles ^c	[0.008, 0.012]	[2.32, 4.10]	[0.72, 1.34]
Sample size = 25, no. of codons per sequence = 500			
Input ^a	0.01	3	2
Mean MLE ^b	0.01	3.53	1.98
Percentiles ^c	[0.003, 0.019]	[1.01, 10.62]	[0.79, 3.36]

For each combination of parameter values, we used the matrix model to generate 200 samples. These samples were analyzed using L_0 (see Equation 12).

^aThe parameter values used to generate random samples.

^bMean value of the maximum-likelihood estimates (MLE).

^cPercentiles [2.5% and 97.5%] of the distributions of the MLEs.

polymorphism can be very selection-like (*i.e.*, P_A and P_a are very different; *e.g.*, Figure 2B), whereas after a population expansion patterns of polymorphism can be more neutral-like (*i.e.*, P_A and P_a are close to 50%; *e.g.*, Figure 1B).

Overall, the L_1 method seems to have substantial power to disentangle selection from demography. This is a useful property because it has long been known that

selection and demography, either acting separately or jointly, can leave very similar traces on polymorphism patterns, and distinguishing them has been a subject of active research (SIMONSEN *et al.* 1995; NIELSEN *et al.* 2005; WILLIAMSON *et al.* 2005; KEIGHTLEY and EYRE-WALKER 2007; ZENG *et al.* 2007).

Applying the new methods to a *D. melanogaster* data set: We used our new methods, L_0 and L_1 , to analyze a

TABLE 3
Performance of the L_1 method in a nonequilibrium population

	θ_b	κ	γ_b	g	τ	Power1 ^d (%)	Power2 ^e (%)
Sample size = 25, no. of codons per sequence = 25,000							
Input ^a	0.004	3	0.4	5	1		
Mean MLE ^b	0.0042	3.06	0.41	5.41	0.94	100	100
Percentiles ^c	[0.0023, 0.0077]	[2.61, 3.65]	[0.26, 0.59]	[3.10, 8.35]	[0.41, 1.32]		
Input ^a	0.02	3	2	0.2	2		
Mean MLE ^b	0.022	2.69	1.86	0.23	1.86	100	100
Percentiles ^c	[0.015, 0.043]	[1.62, 4.57]	[1.30, 2.48]	[0.12, 0.32]	[0.68, 3.73]		
Sample size = 6, no. of codons per sequence = 15,000							
Input ^a	0.004	3	0.4	5	1		
Mean MLE ^b	0.0045	3.42	0.48	5.9	0.90	98	57
Percentiles ^c	[0.0018, 0.0097]	[2.14, 6.23]	[0.06, 1.09]	[3.0, 9.2]	[0.06, 1.87]		
Input ^a	0.02	3	2	0.2	2		
Mean MLE ^b	0.027	3.05	1.9	0.21	2.37	82.1	100
Percentiles ^c	[0.008, 0.095]	[1.41, 9.06]	[1.24, 3.31]	[0.08, 0.44]	[0.73, 5.75]		

In the simulations, we assumed that the population was originally at equilibrium with population size N_b . Then the population size changed instantly to N_a and stayed constant thereafter for t generations, at which point random samples were taken. The parameters were $\gamma_b (= 2N_b s)$, $\theta_b (= 4N_b u)$, κ , $g (= N_a/N_b)$, and $\tau (= t/N_a)$. For each combination of parameter values, 100 replicate simulations were run.

^aThe parameter values used to generate random samples.

^bMean value of the maximum-likelihood estimates (MLE).

^cPercentiles [2.5% and 97.5%] of the distributions of the MLEs.

^dThe power to reject a model with constant population size at a significance level of 5%.

^eThe power to reject neutral evolution at a significance level of 5%.

TABLE 4
Analyzing the twofold degenerate codons using L_0 and L_1

Model		Estimates of parameters					Log-likelihood
		θ_b	κ	γ_b	g	τ	
L_1	MLE	0.0040	1.67	0.50	2.1	780.2	-11627.8
L_0	MLE	0.0083	1.63	1.03	—	—	-11627.8
	95% C.I. ^a	[0.0061, 0.0109]	[1.03, 2.54]	[0.57, 1.48]	—	—	
$L_0(s = 0)^b$	MLE	0.0144	0.60	—	—	—	-11637.7
$L_0(\kappa = 1)^c$	MLE	0.0110	—	0.53	—	—	-11630.1

^aNinety-five percent confidence interval obtained by 250 bootstrap replicates.

^bThe L_0 model with s , the selection coefficient, fixed at zero.

^cThe L_0 model with κ , the mutational bias parameter, fixed at unity.

large *D. melanogaster* polymorphism data set (SHAPIRO *et al.* 2007), summarized in Table 1 (see also MATERIALS AND METHODS).

Initial analysis: The results of the analyses are given in Table 4. Interestingly, the simple model, L_0 , seems to be sufficient to explain the data: there is essentially no increase in the log-likelihood ($\ln L$) when the data were analyzed using L_1 . Further support for this conclusion comes from the fact that, under L_1 , the estimate of the time after expansion, τ , is very large, by which time the population has essentially reached a new equilibrium, and L_1 reduces to L_0 . For this reason, we were unable to obtain a 95% confidence interval under L_1 . Furthermore, consistent with many previous reports (PETROV and HARTL 1999; McVEAN and VIEIRA 2001; NIELSEN *et al.* 2007; KEIGHTLEY *et al.* 2009), the mutational process is not symmetric, but is biased toward preferred-to-unpreferred changes [$L_0(\kappa = 1)$ *vs.* L_0 , $\chi^2 = 4.6$, d.f. = 1, $P = 0.03$]. In contrast, comparing L_0 with the reduced model when the selection coefficient (s) was fixed at zero [*i.e.*, $L_0(s = 0)$ *vs.* L_0], we found strong evidence for recent selection on synonymous codons ($\chi^2 = 19.7$, d.f. = 1, $P = 9.1 \times 10^{-6}$). Using the estimated parameters, the L_0 model can accurately predict the observed data (see Figure S7). In short, the above results suggest that a model with constant population size and selection acting on synonymous codons is a sufficient explanation of the data.

A more detailed analysis: Although the L_0 model seems to provide a rather good fit to the data, it is highly simplified in that it assumes a single selection coefficient and a single mutational bias parameter for all sites. It has been shown by other researchers that different genes can experience different levels of selection pressure, depending on factors such as gene expression level and length of coding region (COMERON and KREITMAN 2002; MASIDE *et al.* 2004; COMERON and GUTHRIE 2005; CUTTER and CHARLESWORTH 2006), and that the mutational bias parameter can be different for different nucleotides (McVEAN and VIEIRA 1999; PETROV and HARTL 1999; KEIGHTLEY *et al.* 2009). We therefore introduced additional parameters into the L_0 model.

First, some of the preferred codons being analyzed differ from their corresponding unpreferred codons by a G to A change at the third codon position, while the rest differ by C to T. We thus extended the model so that each class of codons had its own set of parameters. A maximum-likelihood analysis suggests that this model fits the data much better than the original model ($\chi^2 = 287.0$, d.f. = 3, $P < 10^{-20}$). The MLEs are $\hat{\gamma}_{GA} = 0.85$, $\hat{\gamma}_{CT} = 1.13$, $\hat{\theta}_{GA} = 0.011$, $\hat{\theta}_{CT} = 0.007$, $\hat{\kappa}_{GA} = 0.95$, and $\hat{\kappa}_{CT} = 2.26$ ($\ln L = -11484.3$). However, a model with a common selection coefficient for the two classes of codons fits the data almost equally well ($\chi^2 = 0.34$, d.f. = 1, $P = 0.56$); the MLEs and the log-likelihood under this model are $\hat{\gamma} = 1.03$, $\hat{\theta}_{GA} = 0.010$, $\hat{\theta}_{CT} = 0.008$, $\hat{\kappa}_{GA} = 1.13$, $\hat{\kappa}_{CT} = 2.04$, and $\ln L = -11484.5$. Thus, we assumed that there was no difference in selection coefficient between G/A or C/T ending codons in the following more elaborate analysis.

Another major determinant of codon usage is the level of gene expression (DURET and MOUCHIROUD 1999; HEY and KLIMAN 2002). To model this complication, we used data from the UniGene database (<http://www.ncbi.nlm.nih.gov/unigene>), employing the total number of expressed sequence tags (ESTs) for a gene as a rough measure of its level of expression (the data were kindly provided by B. Vicoso). We divided the genes into two equal-size groups: low-expression and high-expression genes. We allowed each of group of genes to have its own scaled selection coefficient, γ_{low} and γ_{high} , respectively. By fitting the model to the data, we obtained the following MLEs: $\hat{\gamma}_{low} = 0.82$, $\hat{\gamma}_{high} = 1.25$, $\hat{\theta}_{GA} = 0.010$, $\hat{\theta}_{CT} = 0.008$, $\hat{\kappa}_{GA} = 1.14$, $\hat{\kappa}_{CT} = 2.03$, and $\ln L = -11079.3$. This new model further improves the fit to the data compared to $L_0(\mathbf{d} \mid \gamma, \theta_{GA}, \theta_{CT}, \kappa_{GA}, \kappa_{CT})$ ($\chi^2 = 810.3$, d.f. = 1, $P < 10^{-20}$). In accordance with the previous reports, our results suggest that highly expressed genes are under stronger selection pressure than genes with low expression levels.

Finally, we considered the effects of coding region length. We divided low- and high-expression genes, respectively, into two equal-size classes: genes with short and long coding regions. We allowed each group of

genes to have its own selection coefficient. The MLEs are $\hat{\gamma}_{\text{low-short}} = 0.91$, $\hat{\gamma}_{\text{low-long}} = 0.76$, $\hat{\gamma}_{\text{high-short}} = 1.36$, $\hat{\gamma}_{\text{high-long}} = 1.17$, $\hat{\theta}_{GA} = 0.010$, $\hat{\theta}_{CT} = 0.008$, $\hat{\kappa}_{GA} = 1.14$, $\hat{\kappa}_{CT} = 2.04$, and $\ln L = -11068.6$. The improvement in the fit to the data, compared to the model given in the previous paragraph, is also highly significant ($\chi^2 = 21.3$, d.f. = 2, $P = 2.3 \times 10^{-5}$). These results confirm the finding that genes with shorter coding regions tend to be under stronger selection pressure than those with longer coding regions (COMERON *et al.* 1999; DURET and MOUCHIROUD 1999; COMERON and GUTHRIE 2005).

DISCUSSION

The importance of considering nonequilibrium factors in the study of codon usage bias: Population-genetic models of codon usage bias (LI 1987; BULMER 1991; McVEAN and CHARLESWORTH 1999) have mostly assumed that the population is at mutation-selection-drift equilibrium. As evidence for nonequilibrium situations in *Drosophila* species accumulates (TAKANO-SHIMIZU 1999, 2001; KERN and BEGUN 2005; LI and STEPHAN 2006; THORNTON and ANDOLFATTO 2006; STEPHAN and LI 2007), the study of nonequilibrium models has attracted more attention, and some unexpected results have emerged (EYRE-WALKER 1997; TAKANO-SHIMIZU 1999, 2001; COMERON and KREITMAN 2002; COMERON and GUTHRIE 2005; CHARLESWORTH and EYRE-WALKER 2007).

Our matrix model allows systematic studies of the patterns of polymorphism and substitution following a recent change in population size. We were able to confirm and extend the findings reported in the previous studies. Most importantly, we have carried out the first survey of the performance of statistical methods that assume equilibrium in a situation where such an assumption is violated. We can draw two conclusions. First, patterns of polymorphism can be very misleading after a recent change in population size. For example, they can become very neutral-like after a recent population expansion (Figure 1B). In contrast, after a recent population size reduction, patterns of polymorphism are likely to suggest a level of selection pressure higher than the true value (Figure 2B). Second, using statistical methods that assume equilibrium in a nonequilibrium population can result in erroneous inferences of the strength of selection (Figures 3 and 4; see also Figure S5, Figure S6, Figure S8, Figure S9, Figure S10, and Figure S11). These findings indicate that it is important to consider nonequilibrium factors in the study of codon usage bias.

Effects of weak selection on synonymous variants: Contrary to a previous analysis of the same *D. melanogaster* data set (KEIGHTLEY and EYRE-WALKER 2007), we did not find any evidence for a recent population expansion in the Zimbabwe sample. The main difference between the studies is that synonymous sites were

previously assumed to be neutral. However, as shown here, there is evidence for selection on these sites. According to standard population genetics theory, such a selection pressure can result in an excess of low-frequency variants (EWENS 2004, Chap. 5). It is likely that this excess of low-frequency variants was treated by the method of Keightley and Eyre-Walker as the signature of a recent population size expansion. Indeed, when these authors fitted the data using a model with selection on synonymous sites, the support for the expansion event disappeared (see p. 2260 in KEIGHTLEY and EYRE-WALKER 2007). Moreover, recent studies have shown that noncoding regions may be under selection as well (*e.g.*, ANDOLFATTO 2005). These findings suggest that treating certain types of markers as neutral standards can be a dubious procedure, which deserves careful investigation of its validity, whose violation may result in unreliable inferences.

Selection on synonymous codons in *D. melanogaster*:

By analyzing a large polymorphism data set (SHAPIRO *et al.* 2007), we found evidence for natural selection on synonymous codons in *D. melanogaster* (Table 4). Furthermore, we show that genes with shorter coding sequences and/or higher levels of expression are under stronger selection. These results are consistent with previous studies, which suggest that patterns of codon usage bias in *D. melanogaster* are compatible with the operation of selection (KLIMAN 1999; HEY and KLIMAN 2002; CARLINI and STEPHAN 2003; QIN *et al.* 2004; COMERON and GUTHRIE 2005; SINGH *et al.* 2007).

However, a number of studies have also found that selection on synonymous sites may have been substantially reduced in the *D. melanogaster* lineage (AKASHI 1995, 1996; McVEAN and VIEIRA 1999, 2001; NIELSEN *et al.* 2007). A common feature of these studies is that they used between-species divergence data and drew conclusions on the basis of the observation that *D. melanogaster* synonymous sites have fixed significantly more unpreferred alleles than preferred variants (the rates of fixation should be equal at equilibrium). Divergence data can tell us what has happened along the entire *D. melanogaster* lineage, but not when these events happened. To reconcile these findings with ours, we hypothesize that there may have been a reduction in population size in the *D. melanogaster* lineage a long time ago, which resulted in the rapid fixation of many unpreferred variants (*e.g.*, Figure 2A). After this ancient reduction, the population size may have stayed relatively constant, and extant patterns of polymorphism may have come relatively close to the new equilibrium. Because our method does not use divergence data, it has little power to detect such an ancient event, so that the equilibrium model provides a good fit.

The difficulty is that, even if this hypothesis is correct, it is hard to estimate when the reduction in population size occurred, and our method may thus overestimate the current intensity of selection, depending on the

time of the contraction event (see Figure S6). In addition, the potential influences of biased gene conversion (MARAIS *et al.* 2001, 2003; KLIMAN and HEY 2003; MARAIS 2003), changes in the recombinational landscape (TAKANO-SHIMIZU 1999), and recent changes in the mutational processes (TAKANO-SHIMIZU 2001; KERN and BEGUN 2005), as well as the effects of more complex demographic models (*e.g.*, population structure and population bottlenecks), are not considered by our method. Therefore, although there is evidence for selection on synonymous sites, this result should be treated with caution.

Advantages and caveats: The matrix model and the methods developed in this study have a number of advantages. First, the model is highly flexible. Although we focus on the effects of a sudden change in population size here, it is straightforward to modify the model so that it can be used to study effects of more complex demographic models (*e.g.*, population bottlenecks, exponential growth), changes in selection coefficients, and changes in mutational parameters. Second, our methods allow the simultaneous estimation of selection and mutational parameters, in contrast to previous methods that rely only on polymorphic sites (MASIDE *et al.* 2004; CUTTER and CHARLESWORTH 2006). Third, the statistical methods we have proposed do not require the use of an outgroup sequence to infer ancestral *vs.* derived states, a process that is error prone and can lead to unreliable inferences.

There are also some caveats. First, as in most previous studies, we assume that sites are independent. This assumption is obviously unrealistic. Hill–Robertson effects among linked sites might make our methods unreliable (MCVEAN and CHARLESWORTH 2000; COMERON *et al.* 2008). Fortunately, recent simulation studies have suggested that methods assuming free recombination work surprisingly well in practice with relatively free recombination (*e.g.*, with a local recombination rate >2 cM/Mb; K. ZENG, unpublished results; see also WILLIAMSON *et al.* 2005 and BOYKO *et al.* 2008). By using data from highly recombining regions, our results should be robust to the violation of the free-recombination assumption. The second disadvantage of the matrix model is that it is computationally burdensome. In particular, the L_1 model, which requires iterating Equation 5, can be very slow. This is a common problem confronting all studies using matrix models (*e.g.*, KEIGHTLEY and EYRE-WALKER 2007). Despite these caveats, matrix models are flexible and easy to formulate, and their usefulness should not be underestimated.

A computer program implementing the methods described in this article is available from the corresponding author.

We thank Andrea Betancourt, Penny Haddrill, and Peter Keightley for helpful discussions and David Turissini for providing the *Drosophila* data set. We also thank Rasmus Nielsen, John Wakeley, and the anonymous reviewers for their insightful comments. We are very

grateful to the Sun Yat-Sen University Computer Centre for providing computer time and to Hailiang Liu and Haijun Wen for technical support. This work has also made use of the resources provided by the Edinburgh Compute and Data Facility (ECDF) (<http://www.ecdf.ed.ac.uk/>). The ECDF is partially supported by the eScience Data Information and Knowledge Transformation initiative (<http://www.edikt.org.uk>). K.Z. was supported by a Royal Society International Incoming Fellowship. K.Z. also acknowledges support from a National Basic Research Program of China grant (2007CB815701) and a National Natural Science Foundation of China grant (30730008) to Professor Suhua Shi.

LITERATURE CITED

- AKASHI, H., 1994 Synonymous codon usage in *Drosophila melanogaster*: natural selection and translational accuracy. *Genetics* **136**: 927–935.
- AKASHI, H., 1995 Inferring weak selection from patterns of polymorphism and divergence at “silent” sites in *Drosophila* DNA. *Genetics* **139**: 1067–1076.
- AKASHI, H., 1996 Molecular evolution between *Drosophila melanogaster* and *D. simulans*: reduced codon bias, faster rates of amino acid substitution, and larger proteins in *D. melanogaster*. *Genetics* **144**: 1297–1307.
- AKASHI, H., and S. W. SCHAEFFER, 1997 Natural selection and the frequency distributions of “silent” DNA polymorphism in *Drosophila*. *Genetics* **146**: 295–307.
- ANDOLFATTO, P., 2005 Adaptive evolution of non-coding DNA in *Drosophila*. *Nature* **437**: 1149–1152.
- BIERNE, N., and A. EYRE-WALKER, 2006 Variation in synonymous codon use and DNA polymorphism within the *Drosophila* genome. *J. Evol. Biol.* **19**: 1–11.
- BOYKO, A. R., S. H. WILLIAMSON, A. R. INDAP, J. D. DEGENHARDT, R. D. HERNANDEZ *et al.*, 2008 Assessing the evolutionary impact of amino acid mutations in the human genome. *PLoS Genet.* **4**: e1000083.
- BULMER, M., 1991 The selection-mutation-drift theory of synonymous codon usage. *Genetics* **129**: 897–907.
- CARLINI, D. B., and W. STEPHAN, 2003 In vivo introduction of unpreferred synonymous codons into the *Drosophila* Adh gene results in reduced levels of ADH protein. *Genetics* **163**: 239–243.
- CHARLESWORTH, J., and A. EYRE-WALKER, 2007 The other side of the nearly neutral theory, evidence of slightly advantageous back-mutations. *Proc. Natl. Acad. Sci. USA* **104**: 16992–16997.
- COMERON, J. M., and T. B. GUTHRIE, 2005 Intragenic Hill–Robertson interference influences selection intensity on synonymous mutations in *Drosophila*. *Mol. Biol. Evol.* **22**: 2519–2530.
- COMERON, J. M., and M. KREITMAN, 2002 Population, evolutionary and genomic consequences of interference selection. *Genetics* **161**: 389–410.
- COMERON, J. M., M. KREITMAN and M. AGUADE, 1999 Natural selection on synonymous sites is correlated with gene length and recombination in *Drosophila*. *Genetics* **151**: 239–249.
- COMERON, J. M., A. WILLIFORD and R. M. KLIMAN, 2008 The Hill–Robertson effect: evolutionary consequences of weak selection and linkage in finite populations. *Heredity* **100**: 19–31.
- CUTTER, A. D., and B. CHARLESWORTH, 2006 Selection intensity on preferred codons correlates with overall codon usage bias in *Caenorhabditis remanei*. *Curr. Biol.* **16**: 2053–2057.
- DRUMMOND, D. A., J. D. BLOOM, C. ADAMI, C. O. WILKE and F. H. ARNOLD, 2005 Why highly expressed proteins evolve slowly. *Proc. Natl. Acad. Sci. USA* **102**: 14338–14343.
- DURET, L., and D. MOUCHIROUD, 1999 Expression pattern and, surprisingly, gene length shape codon usage in *Caenorhabditis*, *Drosophila*, and *Arabidopsis*. *Proc. Natl. Acad. Sci. USA* **96**: 4482–4487.
- EVANS, S. N., Y. SHVETS and M. SLATKIN, 2007 Non-equilibrium theory of the allele frequency spectrum. *Theor. Popul. Biol.* **71**: 109–119.
- EWENS, W. J., 2004 *Mathematical Population Genetics*. Springer-Verlag, Berlin.
- EYRE-WALKER, A., 1997 Differentiating between selection and mutation bias. *Genetics* **147**: 1983–1987.
- EYRE-WALKER, A., and M. BULMER, 1993 Reduced synonymous substitution rate at the start of enterobacterial genes. *Nucleic Acids Res.* **21**: 4599–4603.

- GALTIER, N., E. BAZIN and N. BIERNE, 2006 GC-biased segregation of noncoding polymorphisms in *Drosophila*. *Genetics* **172**: 221–228.
- GLINKA, S., L. OMETTO, S. MOUSSET, W. STEPHAN and D. DE LORENZO, 2003 Demography and natural selection have shaped genetic variation in *Drosophila melanogaster*: a multi-locus approach. *Genetics* **165**: 1269–1278.
- HADDRILL, P. R., K. R. THORNTON, B. CHARLESWORTH and P. ANDOLFATTO, 2005 Multilocus patterns of nucleotide variability and the demographic and selection history of *Drosophila melanogaster* populations. *Genome Res.* **15**: 790–799.
- HERSHBERG, R., and D. A. PETROV, 2008 Selection on codon bias. *Annu. Rev. Genet.* **42**: 287–299.
- HEY, J., and R. M. KLIMAN, 2002 Interactions between natural selection, recombination and gene density in the genes of *Drosophila*. *Genetics* **160**: 595–608.
- IIDA, K., and H. AKASHI, 2000 A test of translational selection at 'silent' sites in the human genome: base composition comparisons in alternatively spliced genes. *Gene* **261**: 93–105.
- IKEMURA, T., 1981 Correlation between the abundance of *Escherichia coli* transfer RNAs and the occurrence of the respective codons in its protein genes: a proposal for a synonymous codon choice that is optimal for the *E. coli* translational system. *J. Mol. Biol.* **151**: 389–409.
- IKEMURA, T., 1985 Codon usage and tRNA content in unicellular and multicellular organisms. *Mol. Biol. Evol.* **2**: 13–34.
- KAISER, V. B., and B. CHARLESWORTH, 2009 The effects of deleterious mutations on evolution in non-recombining genomes. *Trends Genet.* **25**: 9–12.
- KARLIN, S., and H. TAYLOR, 1975 *A First Course in Stochastic Processes*. Academic Press, New York/London/San Diego.
- KEIGHTLEY, P. D., and A. EYRE-WALKER, 2007 Joint inference of the distribution of fitness effects of deleterious mutations and population demography based on nucleotide polymorphism frequencies. *Genetics* **177**: 2251–2261.
- KEIGHTLEY, P. D., U. TRIVEDI, M. THOMSON, F. OLIVER, S. KUMAR *et al.*, 2009 Analysis of the genome sequences of three *Drosophila melanogaster* spontaneous mutation accumulation lines. *Genome Res.* **19**: 1195–1201.
- KERN, A. D., and D. J. BEGUN, 2005 Patterns of polymorphism and divergence from noncoding sequences of *Drosophila melanogaster* and *D. simulans*: evidence for nonequilibrium processes. *Mol. Biol. Evol.* **22**: 51–62.
- KLIMAN, R. M., 1999 Recent selection on synonymous codon usage in *Drosophila*. *J. Mol. Evol.* **49**: 343–351.
- KLIMAN, R. M., and J. HEY, 2003 Hill-Robertson interference in *Drosophila melanogaster*: reply to Marais, Mouchiroud and Duret. *Genet. Res.* **81**: 89–90.
- LI, H., and W. STEPHAN, 2006 Inferring the demographic history and rate of adaptive substitution in *Drosophila*. *PLoS Genet.* **2**: e166.
- LI, W. H., 1987 Models of nearly neutral mutations with particular implications for nonrandom usage of synonymous codons. *J. Mol. Evol.* **24**: 337–345.
- MARAIS, G., 2003 Biased gene conversion: implications for genome and sex evolution. *Trends Genet.* **19**: 330–338.
- MARAIS, G., D. MOUCHIROUD and L. DURET, 2001 Does recombination improve selection on codon usage? Lessons from nematode and fly complete genomes. *Proc. Natl. Acad. Sci. USA* **98**: 5688–5692.
- MARAIS, G., D. MOUCHIROUD and L. DURET, 2003 Neutral effect of recombination on base composition in *Drosophila*. *Genet. Res.* **81**: 79–87.
- MASIDE, X., A. W. LEE and B. CHARLESWORTH, 2004 Selection on codon usage in *Drosophila americana*. *Curr. Biol.* **14**: 150–154.
- MCVEAN, G. A., and B. CHARLESWORTH, 2000 The effects of Hill-Robertson interference between weakly selected mutations on patterns of molecular evolution and variation. *Genetics* **155**: 929–944.
- MCVEAN, G. A., and J. VIEIRA, 1999 The evolution of codon preferences in *Drosophila*: a maximum-likelihood approach to parameter estimation and hypothesis testing. *J. Mol. Evol.* **49**: 63–75.
- MCVEAN, G. A., and J. VIEIRA, 2001 Inferring parameters of mutation, selection and demography from patterns of synonymous site evolution in *Drosophila*. *Genetics* **157**: 245–257.
- MCVEAN, G. A. T., and B. CHARLESWORTH, 1999 A population genetic model for the evolution of synonymous codon usage: patterns and predictions. *Genet. Res.* **74**: 145–158.
- NIELSEN, R., S. WILLIAMSON, Y. KIM, M. J. HUBISZ, A. G. CLARK *et al.*, 2005 Genomic scans for selective sweeps using SNP data. *Genome Res.* **15**: 1566–1575.
- NIELSEN, R., V. L. BAUER DUMONT, M. J. HUBISZ and C. F. AQUADRO, 2007 Maximum likelihood estimation of ancestral codon usage bias parameters in *Drosophila*. *Mol. Biol. Evol.* **24**: 228–235.
- PETROV, D. A., and D. L. HARTL, 1999 Patterns of nucleotide substitution in *Drosophila* and mammalian genomes. *Proc. Natl. Acad. Sci. USA* **96**: 1475–1479.
- PRESS, W. H., S. A. TEUKOLSKY, W. T. VETTERLING and B. P. FLANNERY, 1992 *Numerical Recipes in C: The Art of Scientific Computing*. Cambridge University Press, Cambridge, UK.
- QIN, H., W. B. WU, J. M. COMERON, M. KREITMAN and W. H. LI, 2004 Intragenic spatial patterns of codon usage bias in prokaryotic and eukaryotic genomes. *Genetics* **168**: 2245–2260.
- SHAPIRO, J. A., W. HUANG, C. ZHANG, M. J. HUBISZ, J. LU *et al.*, 2007 Adaptive genetic evolution in the *Drosophila* genomes. *Proc. Natl. Acad. Sci. USA* **104**: 2271–2276.
- SHARP, P. M., and W. H. LI, 1986 An evolutionary perspective on synonymous codon usage in unicellular organisms. *J. Mol. Evol.* **24**: 28–38.
- SIMONSEN, K. L., G. A. CHURCHILL and C. F. AQUADRO, 1995 Properties of statistical tests of neutrality for DNA polymorphism data. *Genetics* **141**: 413–429.
- SINGH, N. D., P. F. ARNDT and D. A. PETROV, 2005 Genomic heterogeneity of background substitutional patterns in *Drosophila melanogaster*. *Genetics* **169**: 709–722.
- SINGH, N. D., V. L. BAUER DUMONT, M. J. HUBISZ, R. NIELSEN and C. F. AQUADRO, 2007 Patterns of mutation and selection at synonymous sites in *Drosophila*. *Mol. Biol. Evol.* **24**: 2687–2697.
- STEPHAN, W., and H. LI, 2007 The recent demographic and adaptive history of *Drosophila melanogaster*. *Heredity* **98**: 65–68.
- TACHIDA, H., 2000 Molecular evolution in a multisite nearly neutral mutation model. *J. Mol. Evol.* **50**: 69–81.
- TAJIMA, F., 1989 Statistical method for testing the neutral mutation hypothesis by DNA polymorphism. *Genetics* **123**: 585–595.
- TAKANO-SHIMIZU, T., 1999 Local recombination and mutation effects on molecular evolution in *Drosophila*. *Genetics* **153**: 1285–1296.
- TAKANO-SHIMIZU, T., 2001 Local changes in GC/AT substitution biases and in crossover frequencies on *Drosophila* chromosomes. *Mol. Biol. Evol.* **18**: 606–619.
- THORNTON, K., and P. ANDOLFATTO, 2006 Approximate Bayesian inference reveals evidence for a recent, severe bottleneck in a Netherlands population of *Drosophila melanogaster*. *Genetics* **172**: 1607–1619.
- WARNECKE, T., and L. D. HURST, 2007 Evidence for a trade-off between translational efficiency and splicing regulation in determining synonymous codon usage in *Drosophila melanogaster*. *Mol. Biol. Evol.* **24**: 2755–2762.
- WATTERSON, G. A., 1975 On the number of segregating sites in genetical models without recombination. *Theor. Popul. Biol.* **7**: 256–276.
- WILLIAMSON, S. H., R. HERNANDEZ, A. FLEDEL-ALON, L. ZHU, R. NIELSEN *et al.*, 2005 Simultaneous inference of selection and population growth from patterns of variation in the human genome. *Proc. Natl. Acad. Sci. USA* **102**: 7882–7887.
- ZENG, K., S. SHI and C. I. WU, 2007 Compound tests for the detection of hitchhiking under positive selection. *Mol. Biol. Evol.* **24**: 1898–1908.

GENETICS

Supporting Information

<http://www.genetics.org/cgi/content/full/genetics.109.101782/DC1>

Estimating Selection Intensity on Synonymous Codon Usage in a Nonequilibrium Population

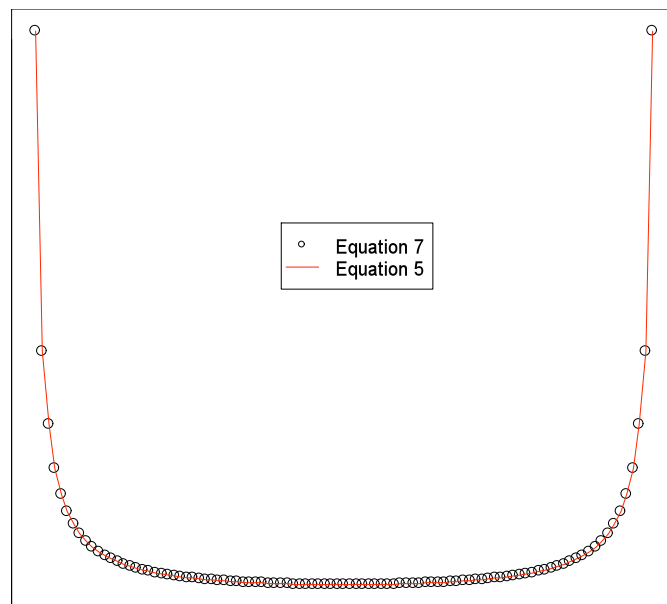
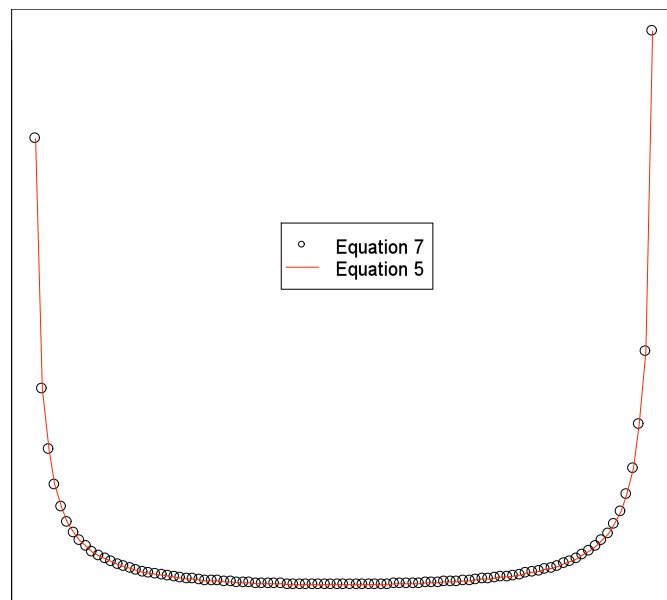
Kai Zeng and Brian Charlesworth

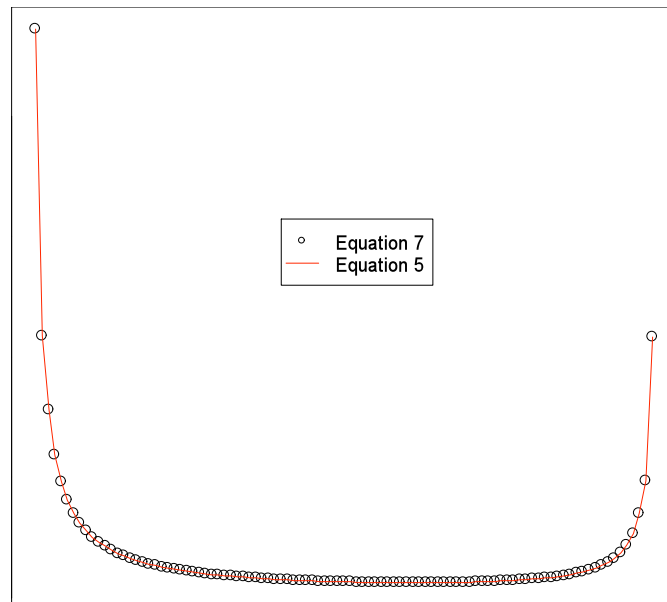
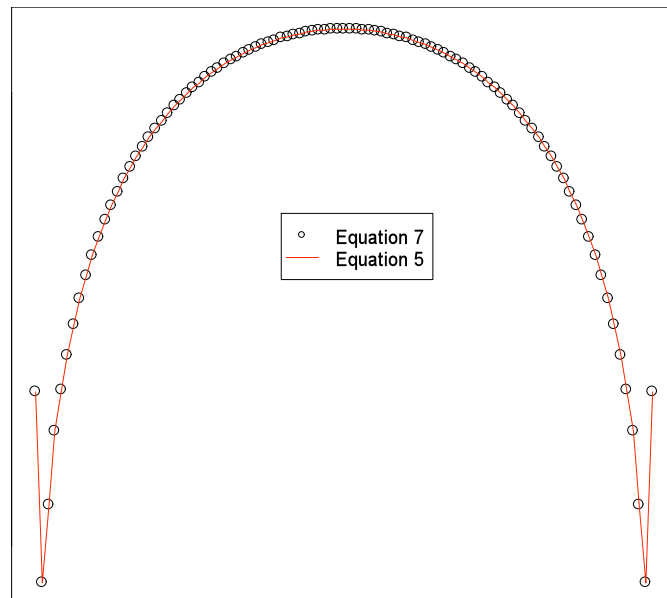
Copyright © 2009 by the Genetics Society of America
DOI: 10.1534/genetics.109.101782

TABLE S1**Dependence of the results on the size of the transition matrix**

Matrix size	Estimates			
	$\mathcal{N}u$	κ	$\mathcal{N}s$	log-likelihood
10	0.003077	0.917820	0.207606	-22611.082430
30	0.002828	0.889085	0.192623	-22589.325861
50	0.002781	0.883834	0.189801	-22588.097341
70	0.002761	0.881730	0.188671	-22587.840626
100	0.002746	0.880115	0.187796	-22587.748956
250	0.002726	0.878012	0.186649	-22587.760553
500	0.002719	0.877235	0.186239	-22587.799641

The analyses were done on a data set of 25 chromosomes and 25,000 codons. This dataset was generated randomly using the parameters $\mathcal{N} = 250$, $u = 10^{-5}$, $\kappa = 1$, $s = 0.001$, i.e., $\mathcal{N}u = 2.5 \times 10^{-3}$ and $\mathcal{N}s = 2.5 \times 10^{-1}$. We used the L_0 method with various sizes of the transition matrix to analyze these data. The estimates of the parameters are shown.

A**B**

C**D**

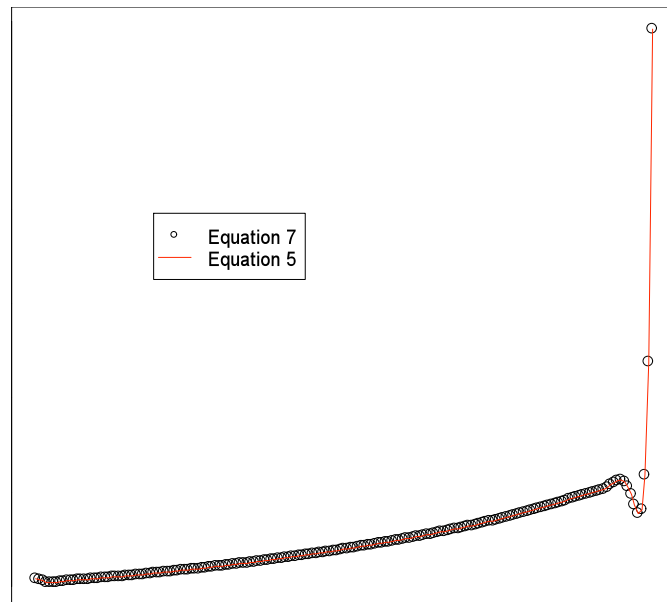
E

FIGURE S1.—Accuracy of Equation 7. We obtained the distribution of the number of polymorphic sites where the unpreferred allele, a , is segregating at various frequencies by either iterating Equation 5, or by using Equation 7. When Equation 7 was used, we obtained the values for the two sub-processes from Equation 8. In (A) – (D), we assumed that the population was composed of 50 diploid individuals, and was at equilibrium. In (E), we assumed that the population was initially at equilibrium with size $N_1 = 100$. Then the population size dropped instantly to $N_2 = 10$. After having a size of 10 for 2 generations (duration = 2), the population size increased instantly to $N_3 = 90$. The distribution of the number of copies of a was investigated at the 4-th generation after the last change in population size.

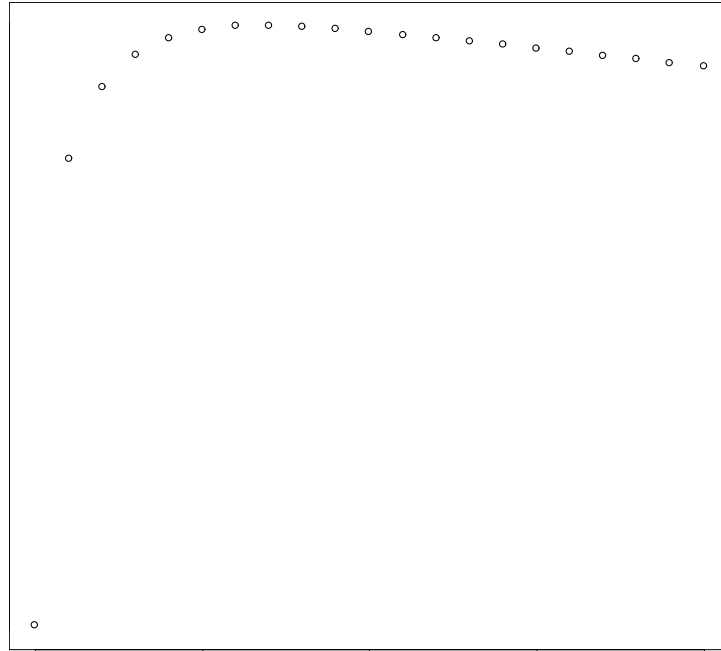


FIGURE S2.—Proportion of sites fixed for A (the preferred allele) after a recent population shrinkage. We assumed that a diploid population of size N_b was originally at equilibrium. At time zero the population size decreased instantly ten-fold to N_a , and stayed constant thereafter. The parameters used to generate this figure were: $\gamma_b = 2N_b s = 2$, $\theta_b = 2N_b u = 0.02$, $\kappa = 3$ (The model and parameters used to generate this figure were the same as those used to generate Figure 2).

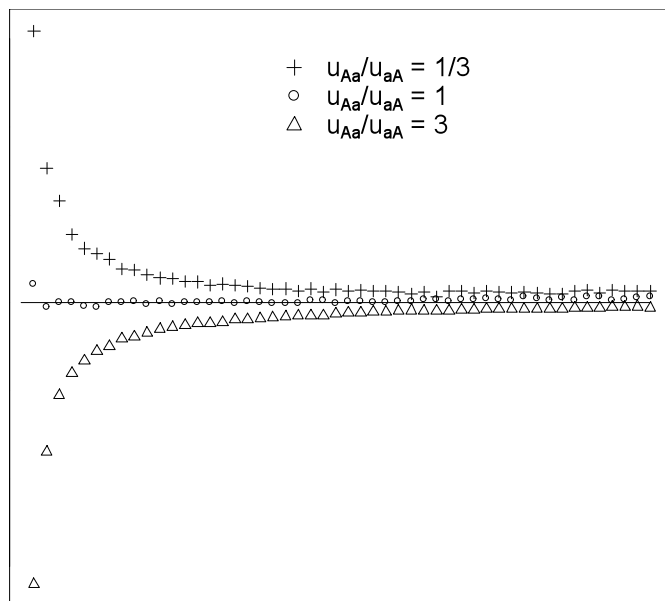


FIGURE S3.—Performance of the MASIDE *et al.* method in the presence of mutational bias. We assumed that the population was at mutation-selection-drift equilibrium. Various levels of selection intensity (γ) were used. The population mutation rate θ was 0.01. Three different levels of mutational bias were simulated: $\kappa = 1/3$, 1, and 3. For each combination of parameter values, 500 random samples of size 15 and 40,000 codons were generated, and were analyzed by the MASIDE *et al.* method. The deviation from the true value of γ was defined as $(E(\gamma_{ml}) - \gamma) / \gamma$ (the y-axis).

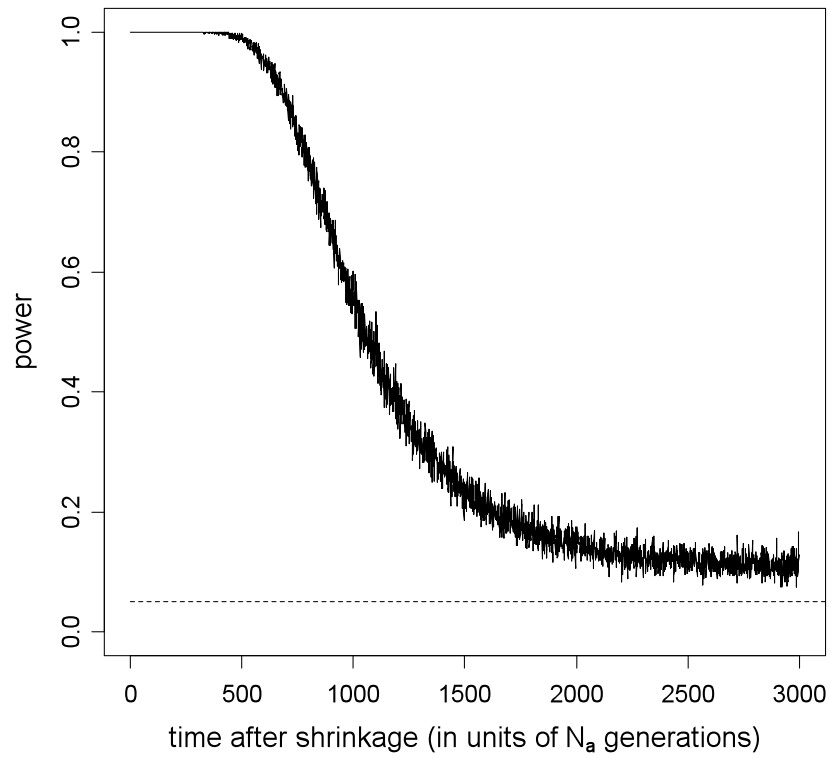
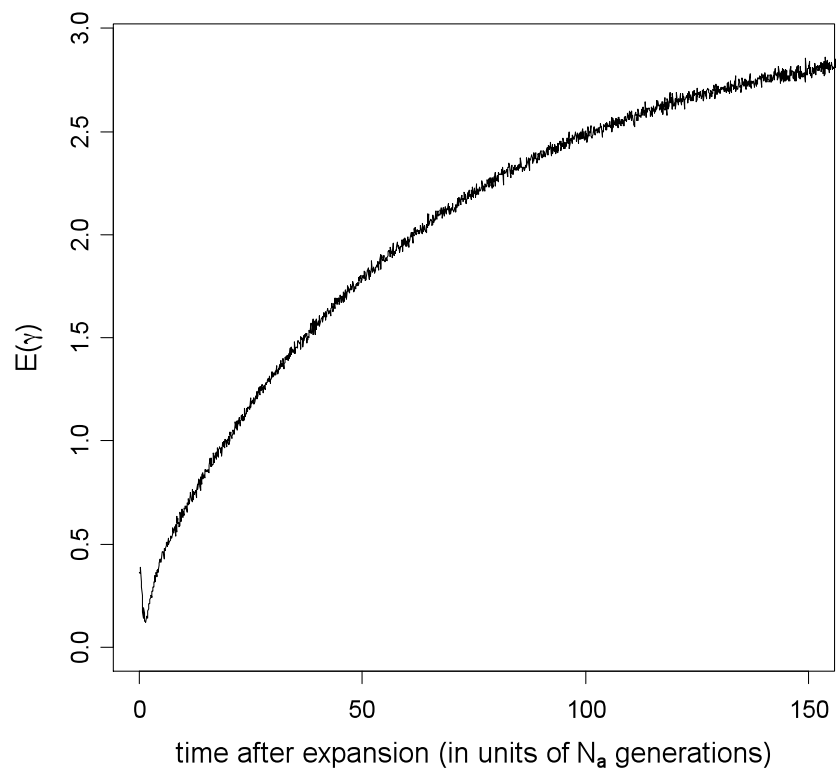
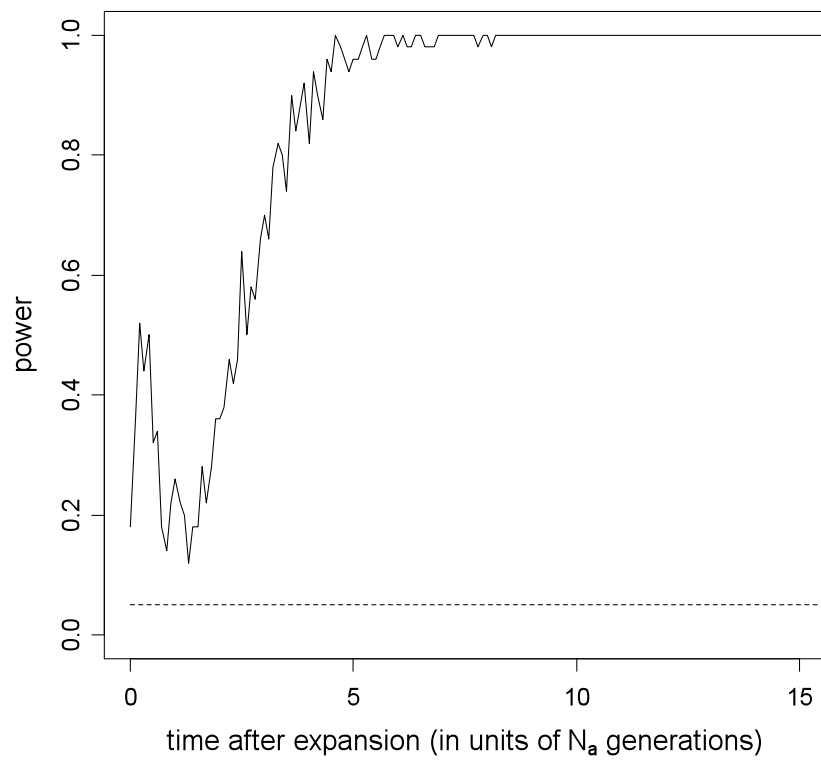


FIGURE S4.—Power of the *MASIDE et al.* method to reject neutrality after a recent population shrinkage. We assumed that a diploid population of size N_b was originally at equilibrium. At time zero the population size decreased instantly ten-fold to N_a , and stayed constant thereafter. The parameters used to generate this figure were: $\gamma_b = 2N_b s = 2$, $\theta_b = 2N_b \mu = 0.02$, $\kappa = 3$ (The model and parameters used to generate this figure were the same as those used to generate Figure 4). The significance level was set to 5%.

A**B**

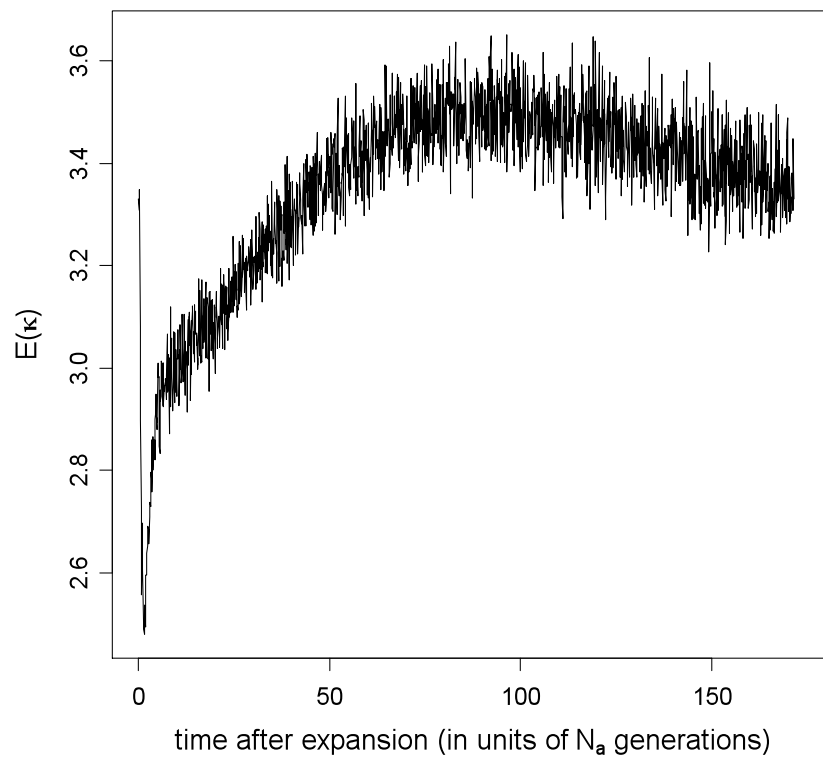
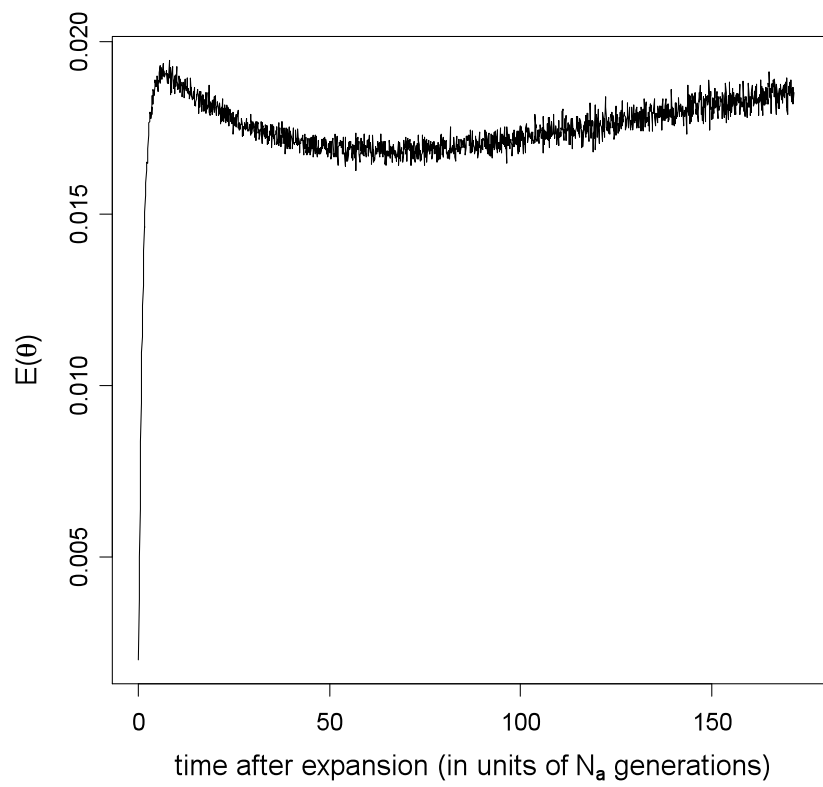
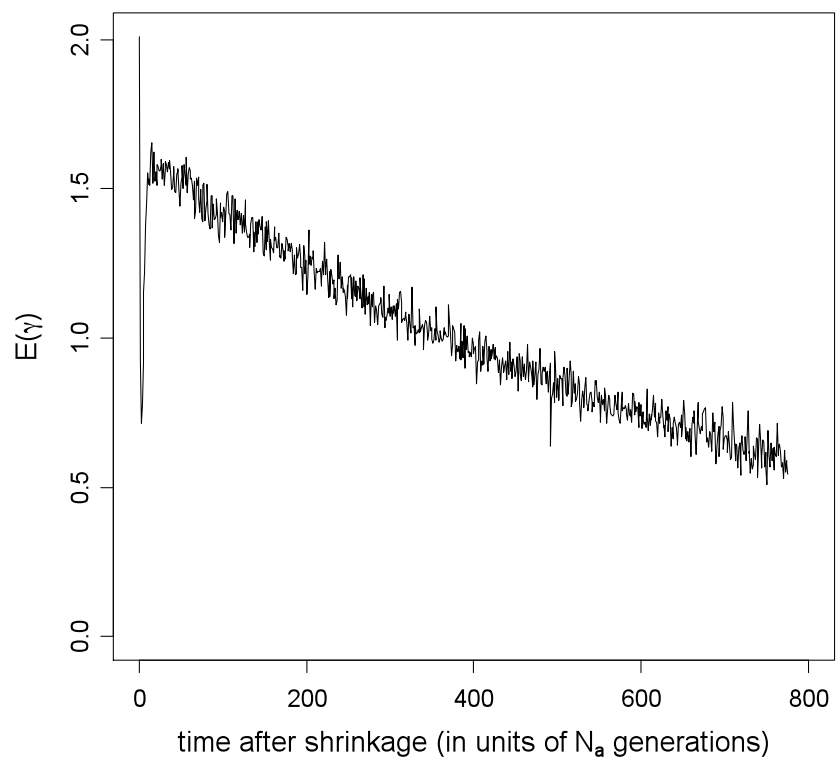
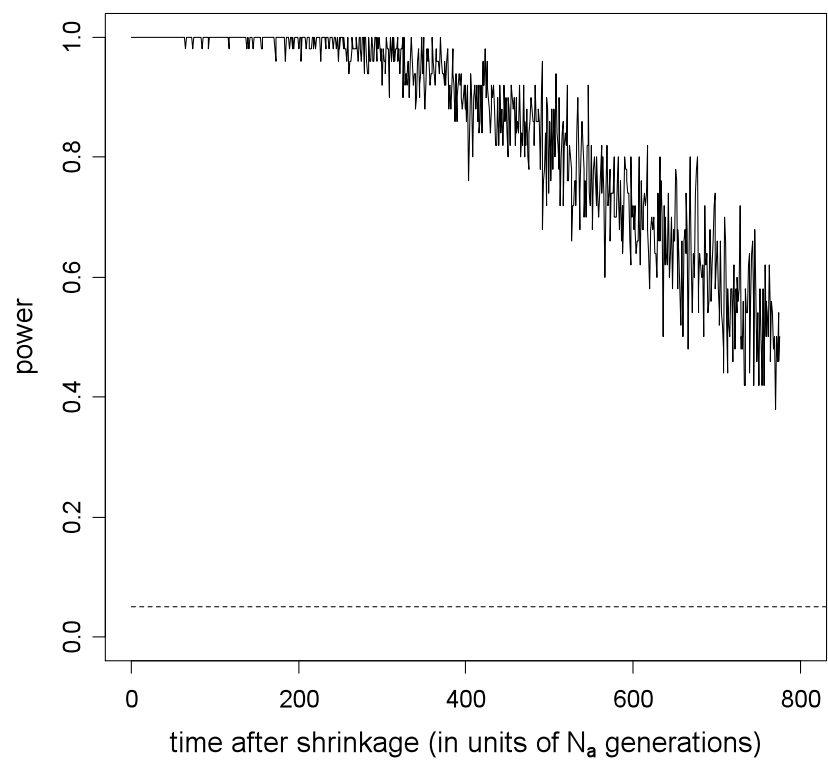
C**D**

FIGURE S5.—Performance of the L_0 method in a population that has experienced a recent size expansion. The model and parameters used to generate this figure were the same as those used to generate Figure 1 (i.e., $\gamma_b = 0.3$, $\theta_b = 0.002$, and $\kappa = 3$). At each time point after the expansion in population size, we randomly generated 50 samples. The sample size was 15, and the total number of codons was 10,000. We then used the L_0 method to analyze each of these samples. (A) The mean values of the estimates of γ . (B) The power to reject neutrality at a significance level of 5%. (C) The mean values of the estimates of κ . (D) The mean values of the estimates of θ . Note that the time scale in (B) is different.

A**B**

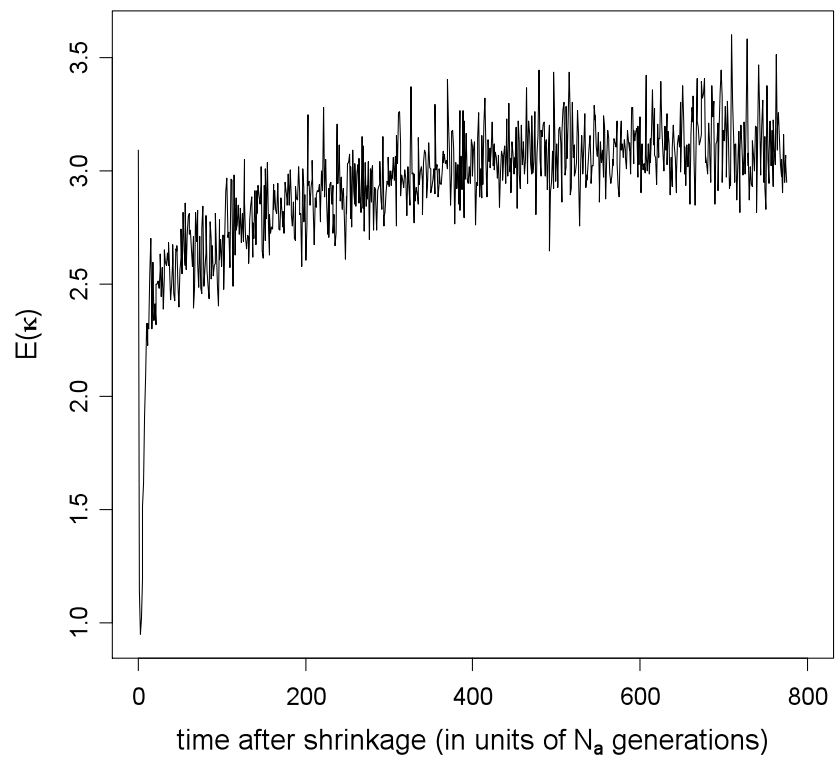
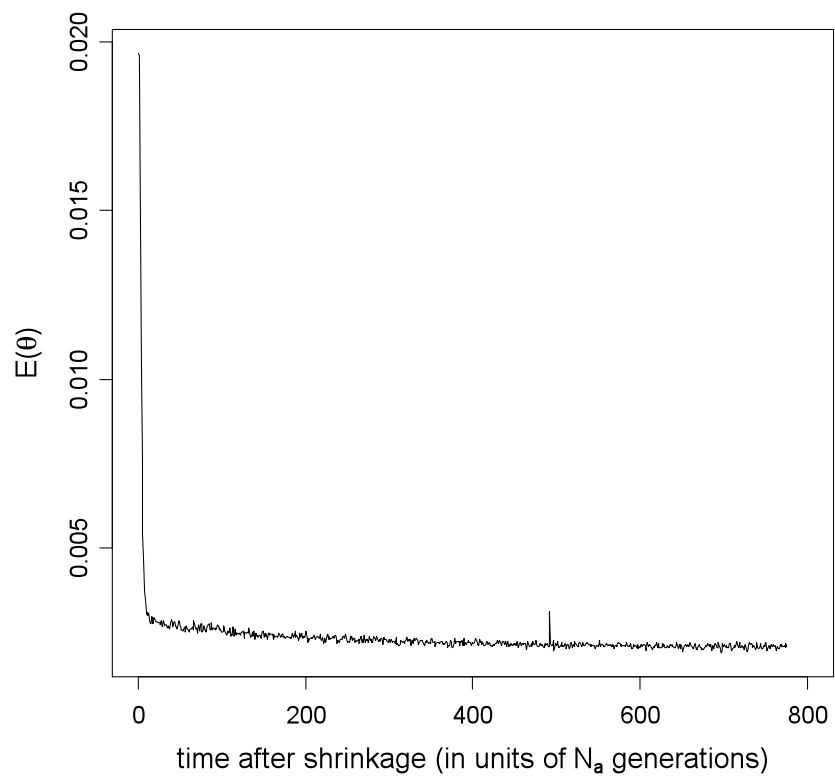
C**D**

FIGURE S6.—Performance of the L_0 method in a population that has experienced a recent size reduction. The parameters used to generate this figure were the same as those used to generate Figure 2 (i.e., $\gamma_b = 2$, $\theta_b = 0.02$, $\kappa = 3$). At each time point after the expansion in population size, we randomly generated 50 samples. The sample size was 15, and the total number of codons was 10,000. We then used the L_0 method to analyze each of these samples. (A) The mean values of the estimates of γ . (B) The power to reject neutrality at a significance level of 5%. (C) The mean values of the estimates of κ . (D) The mean values of the estimates of θ .

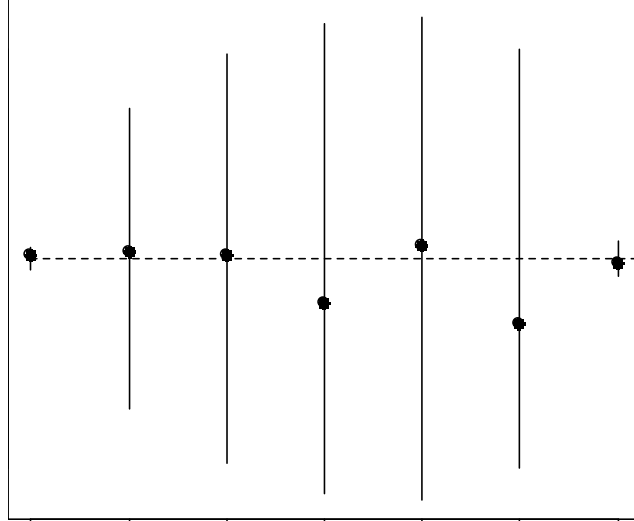


FIGURE S7.—Goodness of fit of the L_0 model to the observed data. The black dots showed the observed values. The lines extending from each black dot indicated the 95% confidence interval. In the y-axis, *exp* means the expected value, and *obs* means the observed value.

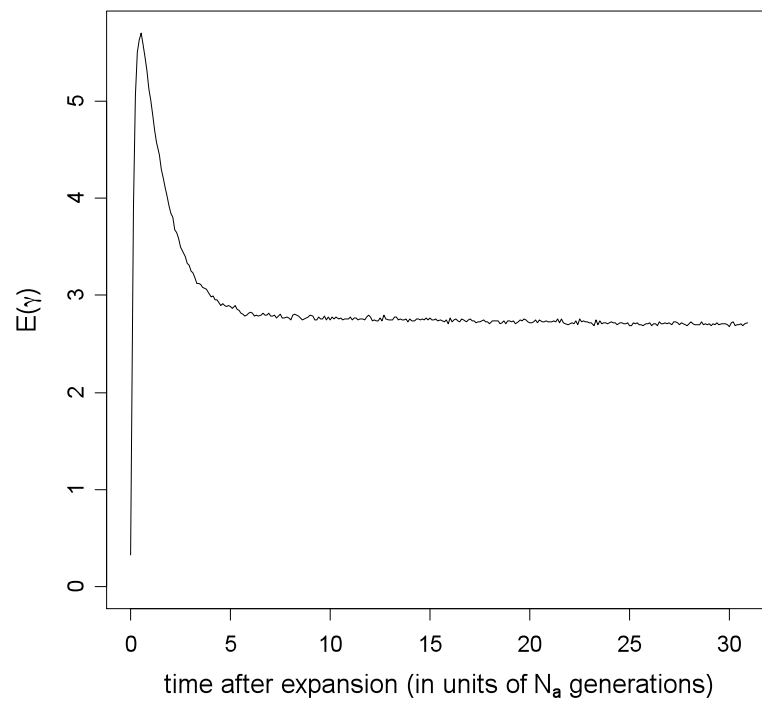
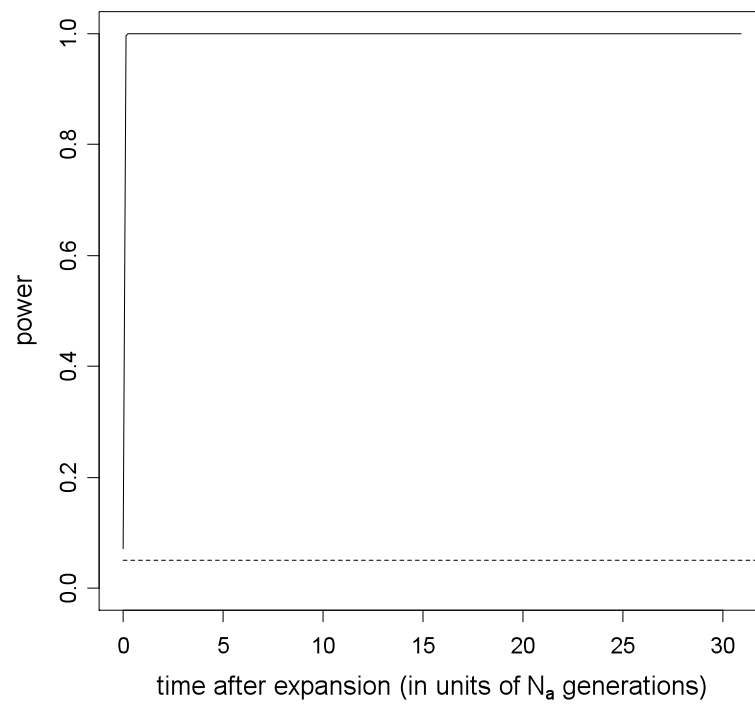
A**B**

FIGURE S8.—Performance of the Akashi-Schaeffer method in a population that has experienced a recent size expansion. The model and parameters used to generate this figure were the same as those used to generate Figure 1 (i.e., $\gamma_b = 0.3$, $\theta_b = 0.002$, and $\kappa = 3$). At each time point after the expansion in population size, we randomly generated 500 samples. The sample size was 15, and the total number of codons was 10,000. We then used the Akashi-Schaeffer (1997) method to analyze each of these samples. Note that we only used the preferred-to-unpreferred mutations in the analysis. (A) The mean values of the estimates of γ . (B) The power to reject neutrality at a significance level of 5%.

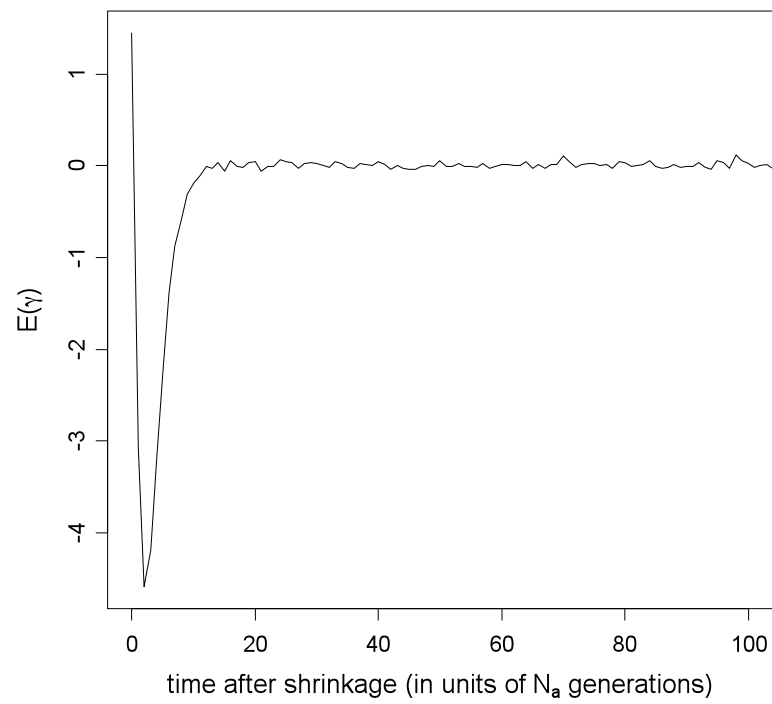
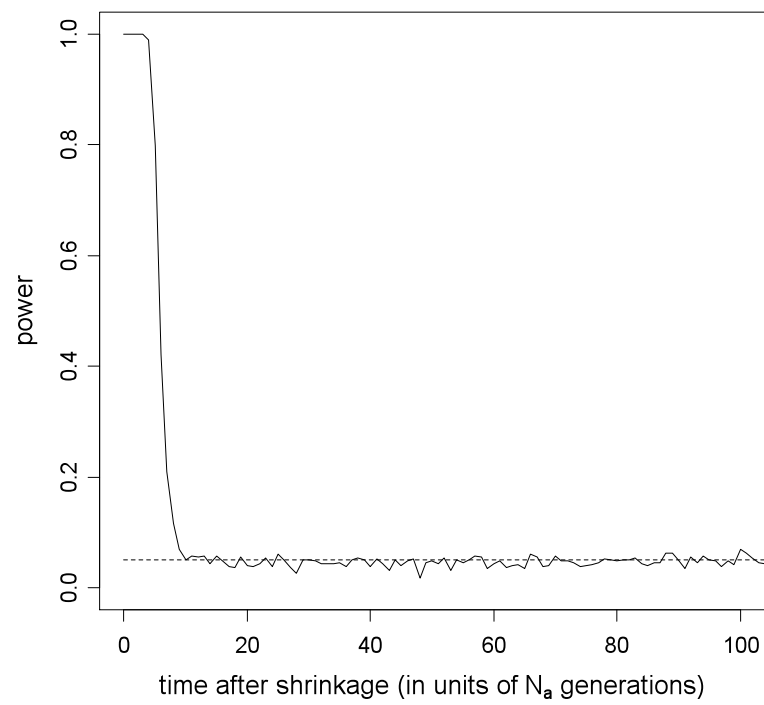
A**B**

FIGURE S9.—Performance of the Akashi-Schaeffer method in a population that has experienced a recent size reduction. The parameters used to generate this figure were the same as those used to generate Figure 2 (i.e., $\gamma_b = 2$, $\theta_b = 0.02$, $\kappa = 3$). At each time point after the expansion in population size, we randomly generated 500 samples. The sample size was 15, and the total number of codons was 10,000. We then used the L_0 method to analyze each of these samples. Note that we only used the preferred-to-unpreferred mutations in the analysis. (A) The mean values of the estimates of γ . (B) The power to reject neutrality at a significance level of 5%.

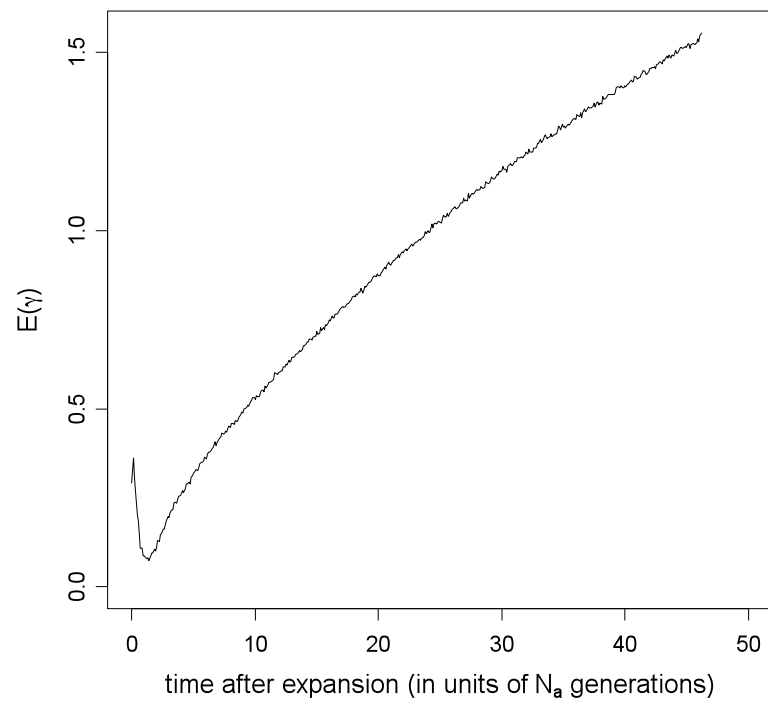
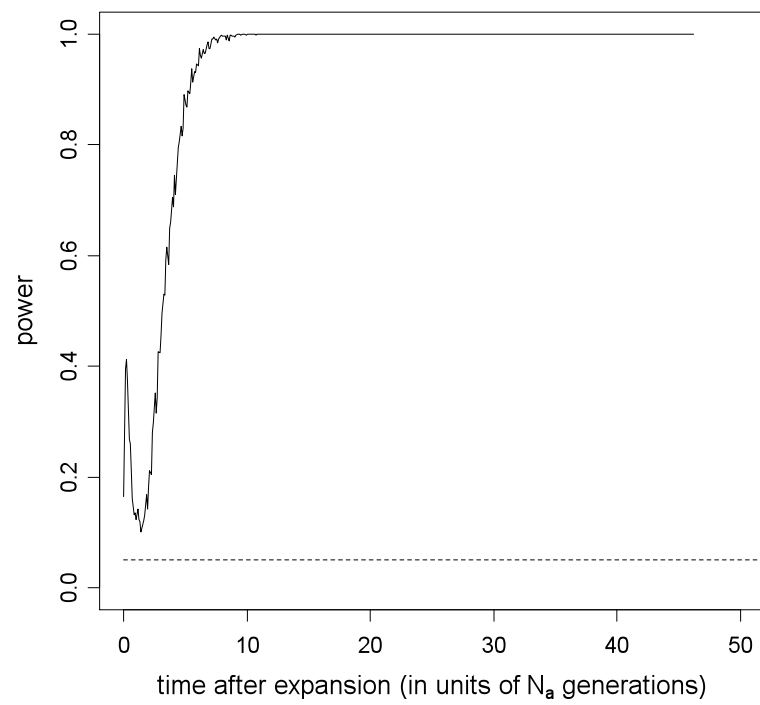
A**B**

FIGURE S10.—Performance of the Cutter-Charlesworth method in a population that has experienced a recent size expansion. The model and parameters used to generate this figure were the same as those used to generate Figure 1 (i.e., $\gamma_b = 0.3$, $\theta_b = 0.002$, and $\kappa = 3$). At each time point after the expansion in population size, we randomly generated 500 samples. The sample size was 15, and the total number of codons was 10,000. We then used the Cutter-Charlesworth method to analyze each of these samples. (A) The mean values of the estimates of γ . (B) The power to reject neutrality at a significance level of 5%.

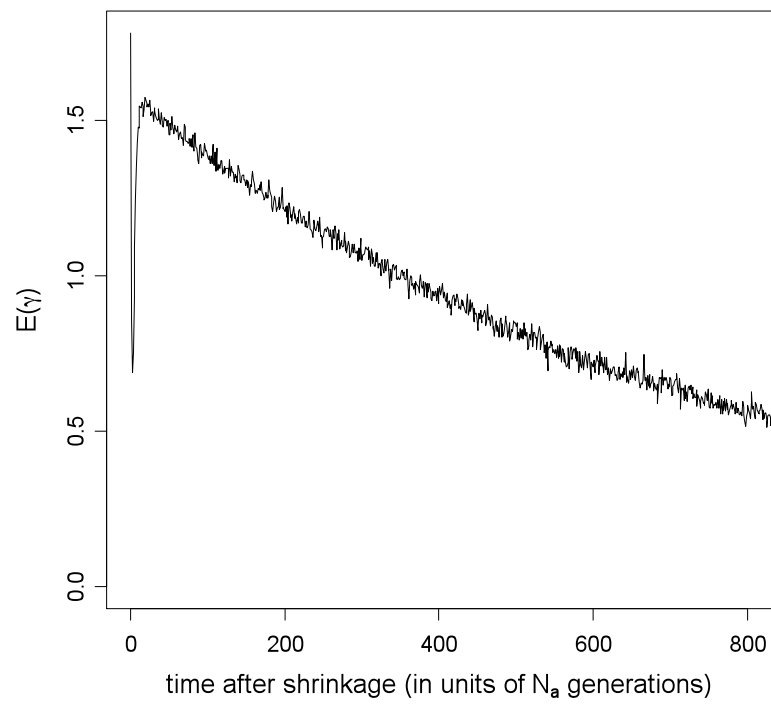
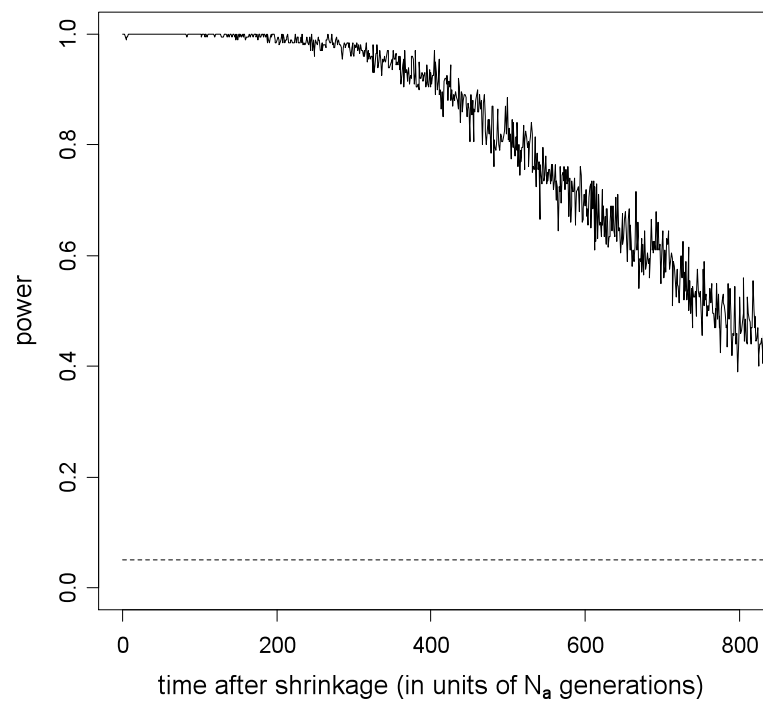
A**B**

FIGURE S11.—Performance of the Cutter-Charlesworth method in a population that has experienced a recent size reduction. The parameters used to generate this figure were the same as those used to generate Figure 2 (i.e., $\gamma_b = 2$, $\theta_b = 0.02$, $\kappa = 3$). At each time point after the expansion in population size, we randomly generated 500 samples. The sample size was 15, and the total number of codons was 10,000. We then used the Cutter-Charlesworth method to analyze each of these samples. (A) The mean values of the estimates of γ . (B) The power to reject neutrality at a significance level of 5%.